

**Aus der  
Radiologischen Universitätsklinik Tübingen  
Abteilung Radiologische Diagnostik  
Ärztlicher Direktor: Professor Dr. C. D. Claussen**

**Coronary Angiography with Four-row Multidetector  
Computed Tomography**

**Inaugural-Dissertation  
zur Erlangung des Doktorgrades  
der Medizin**

**der Medizinischen Fakultät  
der Eberhard-Karls-Universität  
zu Tübingen**

**vorgelegt von**

**Jens Martensen**

**aus Hørsholm, Dänemark**

**2005**

**Dekan: Professor Dr. C. D. Claussen**

**1. Berichterstatter: Professor Dr. C. D. Claussen**

**2. Berichterstatter: Professor Dr. M. Hofbeck**

To

**Romana**

and our daughter

**Nora-Mia**

# Contents

<b>1. Introduction .....</b>	<b>4</b>
1.1. Challenges in Non-invasive Cardiac Imaging .....	5
1.2. Computed Tomography in Cardiac Imaging .....	6
1.2.1. Conventional CT.....	6
1.2.2. Electron Beam CT .....	6
1.2.3. Spiral CT .....	8
1.2.4. Multi-Row Spiral CT .....	8
1.3. Coronary Artery Disease.....	9
1.4. Study Objective.....	11
<b>2. Methods .....</b>	<b>12</b>
2.1. Study Design .....	12
2.2. MDCT Angiography .....	13
2.3. Post Processing and Image Reconstruction .....	16
2.4. Image Artefacts.....	18
2.5. Image Display .....	21
2.6. Ca-scoring .....	22
2.7. Conventional Angiography with Quantitative Coronary Analysis .....	22
2.8. Data Evaluation and Statistics .....	23
<b>3. Results .....</b>	<b>26</b>
3.1. Study Population.....	26
3.2. Detection of Coronary Lesions by CTA and CCA. ....	26
3.3. Influencing Factors for CTA Performance.....	27

3.3.1. Lesion Size.....	28
3.3.2. Lesion Location Within the Coronary Tree .....	29
3.3.3. Heart Rate .....	32
3.3.4. Coronary Calcium.....	34
3.3.5. Summery of Results .....	36
3.4. Influence of Contrast Media on Patient Heart Rate.....	38
3.5. Image Examples .....	42
<b>4. Discussion .....</b>	<b>44</b>
4.1. Limitations of CTA as a Diagnostic Tool for CAD .....	44
4.2.1. Heart Rate .....	45
4.2.2. Lesion Size .....	47
4.2.3. Lesion Location Within the Coronary Tree.....	48
4.2.4. Coronary Calcium .....	49
4.3. Soft Plaque .....	52
4.4. Influence of Contrast Media on Patient Heart Rate.....	53
4.5. Limitation of the Study .....	54
4.6. Prospects of coronary CTA.....	56
<b>5. Summary.....</b>	<b>57</b>
<b>6. Appendage .....</b>	<b>59</b>
6.1. Raw Data .....	59
<b>7. References .....</b>	<b>72</b>

# Abbreviations

acq	Acquisition
CABG	Coronary Artery Bypass Graft
CAD	Coronary Artery Disease
CCA	Conventional Coronary Angiography
CT	Computer Tomography
CTA	Computed Tomography Angiography
EBCT	Electron Beam Computer Tomogra
I	Iodine
kV	Kilovolt
LAD	Left Anterior Descending Branch
LAO	Left Anterior Oblique Projection
LCA	Left Coronary Artery
LCX	Left Circumflex Branch
LM	Left Main
mA	Milliampere
MDCT	Multi-Detector Computer Tomography
MI	Myocardial Infarction
MIP	Maximum Intensity Projection
ml	milliliter
mm	millimeter
MRI	Magnetic Resonance Imaging
ms	millisecond
PTCA	Percutaneous Transluminal Coronary Angioplasty
RAO	Right Antrior Oblique Projection
rot	Rotation
t	Time

# 1. Introduction

Coronary heart disease is the most common cause of death in Europe, accounting for nearly 2 million deaths each year. Over one in five women (22%) and men (21%) die from this disease (82).

For a number of years CCA has been without competition in the diagnosis of coronary heart disease, since it is the only established method by which stenosis of coronary vessels can be directly visualized. Furthermore, CCA offers the option of treatment through PTCA and stent implantation. With over 4000 procedures performed per one million inhabitants, Germany is the European country in which the highest number of conventional coronary angiograms is performed (26).

The drawbacks of CCA, like its advantages, are inherent to the invasive nature of the procedure. Catherization involves considerable discomfort for the patient and complications ranging from hemorrhage at the site of catheter insertion to coronary rupture may occur. Although severe complications are rare, the risk involved with CCA usually requires a short hospitalization of the patient (56). These drawbacks of CCA must be considered when defining the indication for the procedure, limiting the procedure to high risk patients and patients who already show symptoms of CAD (85).

In recent years attempts to develop a non-invasive modality for the detection and visualization of coronary artery stenoses have been made. A modality involving only low patient risk would open the possibility of examining a much larger population of patients. Ideally, such a modality could be used to screen for CAD, resulting in earlier detection, and thus more effective treatment of the disease.

## 1.1. Challenges in Non-invasive Cardiac Imaging

The most eminent challenge in non-invasive coronary angiography is image distortion caused by motion. The coronary vessels are not alone subjected to the rapid and often irregular motion of the heart, but also to motion caused by breathing. The adverse effect of breathing merely presents a minor obstacle in coronary angiography since it may be avoided simply by voluntary patient breath hold. In this case the acquisition of the images is limited to the given time window of patient breath hold which is usually no longer than 40 seconds.

Cardiac motion presents the greatest challenge in coronary angiography. Naturally, the motion of the heart may be controlled by pharmacological substances such as  $\beta$ -blockers, but adequate depiction of the coronaries is challenging even at slow and steady heart rates.

To overcome the obstacle of cardiac motion, modalities for cardiac imaging must be capable of image acquisition with fast temporal resolution. Otherwise, motion artifacts will occur, rendering the images unusable for diagnostic purposes.

Another mandatory requirement in coronary angiography is sufficient spatial resolution for the adequate depiction of the small coronary vessels and the plaques that may be present within the vessel walls.

Furthermore, non-invasive coronary angiography requires of high contrast resolution in order to properly differentiate the vessel lumen from surrounding tissue. Contrast media may be applied in order to opacify the lumen of coronary structures. But in non-invasive angiography the contrast agent is applied systemically, limiting the possibility of achieving high opacification of the coronary vessels.

Only few imaging modalities such as cardiac MRI, EBCT and MDCT possess the combination of qualities required for non-invasive coronary angiography. Currently, no non-invasive image modality has managed to fully overcome the challenges presented in coronary angiography and CCA remains the gold standard for the detection of CAD.



## 1.2. Computed Tomography in Cardiac Imaging

### *1.2.1. Conventional CT*

X-ray computed tomography was first introduced in 1972 when Dr. Godfrey Hounsfield and James Ambrose successfully diagnosed a brain tumor in a 41 year old woman. In conventional CT a rotating x-ray source emits ionizing radiation of a defined beam shape and thickness. The beam passes through the patient at numerous projections and the resulting variations in radiation is registered by detectors located opposite the radiation source. A two-dimensional image of a given thickness can be mathematically derived from the data of these numerous projections. When an image has been acquired, the patient is advanced to an adjacent location and the process is repeated, this procedure is known as step-and-shoot. The contrast resolution of the resulting images is far superior to that of conventional radiography. But the limited temporal resolution of conventional CT systems does not permit adequate imaging of rapidly moving organs such as the heart (51).

### *1.2.2. Electron Beam CT*

In 1982 electron beam CT (EBCT) was introduced, presenting a dedicated modality for cardiac imaging. EBCT is capable of very fast image acquisition since the source of radiation is not placed on a rotating gantry but is stationary. The emitted electron beam sweeps across a semi circular tungsten anode target, emitting an x-ray fan-beam which is detected by an array of photodiodes opposite the tungsten target. With this technique, the data acquisition time is not limited by the G-force which occurs with gantry rotation and temporal resolution of 50 – 100ms becomes possible.

This leap in technology permitted motion free non-invasive coronary imaging. EBCT, however, did not manage to deliver consistently reliable results in patients with variations of heart rate. Furthermore, EBCT technology is very costly and therefore is only available at few institutions (1,3,14,23,50,65,68,83).

EBCT coronary angiography depends on prospective ECG triggering in order to obtain images from the diastole part of the cardiac cycle in which the least amount of motion occurs. With this method, the ECG-trace of the patient is used to trigger the scan at a certain reader defined time period after each R-wave (73). Although very good results were obtained with this method, some EBCT studies showed significant motion artifacts despite the fast temporal resolution, revealing new challenges obtaining to cardiac movement (6,50). With prospective ECG-triggering the interval of image acquisition must be defined in advance with the risk of obtaining images that are not free of motion. Furthermore, the heart has a unique motion pattern and the optimal time of image reconstruction varies for each coronary branch. It may occur that a set of images from the same phase of the cardiac cycle depict one coronary branch free of motion artifacts while another branch is distorted (4,37).

Prospective ECG-triggering has proven to be very sensitive to variations in cardiac rhythm. The prospective nature of the method by which the scan interval is initiated at a fixed delay after the R-wave does not adapt to variation in length of the R-R interval. If such variations occur, the data sample may well fall within the systole phase of the cardiac cycle, resulting in extensive image artifacts caused by cardiac motion (77).

### *1.2.3. Spiral CT*

The next technological leap took place in the early 90's with the introduction of spiral CT. With this technology the gantry containing the x-ray tube and a series of detectors rotates continually around the patient. The patient is situated on a table which is advanced through the gantry at a given speed known as 'pitch', defined as table feed per gantry rotation divided by the collimated slice thickness. By this method, a continuous spiral of three-dimensional image data covering all positions in the longitudinal axis is generated. Axial images are calculated by linear interpolation of the spiral data. This method results in a substantial improvement of temporal resolution resulting from the faster gantry rotation speed which is possible due to continuous gantry rotation (51,52)

Single slice spiral CT has become a reliable and widely applied non-invasive imaging modality in vascular diagnostics but does not offer the combined merits of temporal and spatial resolution necessary for non-invasive coronary angiography (53,77,80,81,84).

### *1.2.4. Multi-Row Spiral CT*

Multi-row spiral CT is the latest evolution of spiral CT technology, offering a notable increase in spatial and temporal resolution. With this method a continually rotating gantry contains multiple detector rows opposite a single x-ray tube. This enables the simultaneous acquisition of several images per gantry rotation. Additionally, modern multi row systems operate with gantry rotation times of 500 ms and below, while most single slice scanners are not capable of sub-second gantry rotation.

A four-row MDCT system with 500ms gantry rotation time, as used in this study, is capable of scanning a given volume with a fixed collimation eight times faster than a single slice system with one second gantry rotation. This eight fold increase of potential is derived from the four times wider field of data acquisition at half the gantry rotation time.

The increase of potential can also be utilized to scan a given volume within the same time as the single slice scanner, but with eight times the spatial resolution (51,77).

With this new generation of CT scanners the entire volume of the heart can be scanned with adequate spatial resolution within the time of a single breath hold, eliminating breathing artifacts. The temporal resolution of 250ms is fast enough to permit motion free imaging within the diastole part of cardiac cycle (74).

The most significant advantage of multi-row CT over EBCT is the possibility of acquiring data sets with continuous volume coverage of the heart (74). When this data is synchronized with the patient ECG-signal, retrospective image reconstruction at any given phase of the cardiac cycle is possible, since image data from all phases of the cardiac cycle is available. Retrospective gating of the image reconstruction intervals is much less sensitive to variations in cardiac rhythm because any given variations are now known at the time of image reconstruction (77). The prospective gating method used in EBCT coronary angiography is not able to predict such variations of cardiac rhythm (6).

### 1.3. Coronary Artery Disease

The physical manifestation of Coronary artery disease is the presence of atherosclerotic lesions within the walls of coronary arteries. These Lesions are known as plaque. As CAD progresses, the growing plaque cause a narrowing of the coronary lumen and the blood flow to the myocardium is compromised. The resulting myocardial ischemia is the cause of the commonly known angina symptoms (chest pain, pain in left shoulder and arm, shortness of breath etc.) These symptoms typically occur during physical activity when the oxygen metabolism of the myocardium is increased. An increase supply of oxygenated blood is hindered by the stenosis within the given coronary artery and myocardial ischemia occurs.

Certain types of coronary plaque tend to rupture causing acute thrombotic occlusion of the vessel lumen. In this case, the ischemia is not reversible and necrosis of the ischemic myocardium occurs. This situation is often fatal, depending on the extent and location of damaged myocardium.

The risk factors of CAD are commonly known as high blood pressure, high blood levels of low density lipoprotein, smoking, diabetes, obesity, lack of exercise and genetic disposition (10,11,27).

Not all aspects of plaque formation have yet been revealed, but Inflammation caused by endothelial injury probably plays a major role in the development of CAD (78). Atherosclerotic plaque consists of two major components: Atheromatous tissue which is rich in lipids and of a soft consistency and sclerotic tissue which is collagen-rich and hard. It is generally believed that macrophage foam cells present within atherosclerotic plaque are responsible for the accumulation of extracellular lipid at the core of the lesion. Inflammation causes an increase in macrophage activity resulting in growth of the lipid core of the plaque. As the lipid core grows, the lesion becomes more unstable and prone to rupture (20). In general, soft plaque does not tend to compromise the lumen of the vessel greatly, since they contain little of the voluminous sclerotic tissue found in more stable plaque. None the less, these soft plaques are responsible for most acute coronary events, since they are prone to rupture causing thrombotic occlusion of the vessel (29,87,96).

Organization of the plaque takes place when collagen is secreted by smooth muscle cells, stabilizing the structure of the plaque. During plaque organization, mineralization (calcification) may occur, causing further stabilization the structure (28,48,97). Organized coronary lesions may cause extensive narrowing of the vessel lumen, resulting in myocardial ischemia and angina pain. The progression of stable plaque is often relatively slow, allowing collateralization of the diseased vessel. Because of their stable structure, organized lesions do not rupture as often as soft plaque (95).

Coronary angiography depicts the lumen of coronary arteries, thereby showing luminal narrowing when plaque is present. The depiction of coronary stenoses is a direct proof CAD.

## 1.4. Calcium Scoring

Due to the high contrast resolution of computed tomography, detection and quantification of calcium within the walls of coronary arteries is possible. EBCT has proven to be a very strong tool for calcium scoring, and numerous studies have been performed on this subject (13,15,17,21,22,43). While there is no question that coronary calcification occurs in the process of CAD, there has been much controversy as to the meaning of coronary calcium as a predicting factor for future coronary events (41,49,55,70). The presence of coronary calcium does not always coincide with coronary lumen narrowing and coronary plaque is not always calcified (79,95). It has been shown that calcium within a coronary plaque is a sign of organization and stabilization of the lesion, making calcified plaque less likely to rupture causing an acute coronary event (28,48,97).

## 1.4. Study Objective

This study aims to analyse the potential of four-row MDCT coronary angiography for the detection of stenotic coronary lesions by comparing the results of CTA to a gold standard set by CCA.

A further analysis of these results accounting for heart rate, coronary calcification, lesion size and motion pattern of each separate coronary arteries was performed with the objective of demonstrating the interfering influence of these factors.

## 2. Methods

### 2.1. Study Design

The 70 patients included in this study all underwent conventional and MDCT angiography of the coronary arteries. Principally, all patients scheduled for conventional coronary angiography were eligible for participation. Criteria of exclusion were: renal insufficiency (creatinine > 2.5 mg/dl), instable angina, acute MI, previous CABG-Operation, known allergy to contrast media, claustrophobia, and exposure to levels of radiation above 5 mSv in the past 12 month. The study protocol was approved by the hospitals ethics committee and all patients gave informed consent.

Initially the CTA examination was performed and the reconstructed images were evaluated by an on staff radiologist. 1 – 2 days after the CTA scan the scheduled CCA examination took place. The evaluation of the CCA examination was performed by a physician blinded to the results of CTA. At a later point in time the results of CCA were validated by quantitative coronary analysis (QCA). The location and extent of each diagnosed coronary lesion was recorded separately for each modality.

Finally a comparative analysis of CCA and CTA results was performed, yielding sensitivity, specificity, positive and negative predictive value of CTA compared with CCA.

The influence of potentially interfering factors such as heart rate, coronary calcification, lesion size and motion pattern of the coronary arteries was demonstrated in a separate evaluation.

In order to demonstrate how the intravenous application of non-ionic contrast media might influence patient heart rate, a comparative analysis of the mean heart rates of the 70 patients during the native and the contrast enhanced scan was performed.

The following chapters describe each performed procedure in further detail.

## 2.2. MDCT Angiography

All patients were examined with a MDCT scanner (Somatom Plus 4 Volume Zoom, Siemens Ag, Erlangen, Germany) which is capable of acquiring 4 slices per gantry rotation. The patients ECG signals were recorded simultaneous to each spiral CT scan, so that the acquired image data from each scan could be matched to a specific phase of the cardiac cycle. Images from any given phase of the cardiac cycle could then be reconstructed during post processing.

Initially a native MDCT scan was performed with a detector collimation of  $4 \times 2.5$  mm. These images were used to determine the scan volume and the correct anatomical location for detection of the timing bolus.

The timing bolus was given in order to determine the individual circulation delay between the time of contrast injection and the time of maximum opacification in the ascending aorta. The bolus (20ml iodinated contrast agent, 400 mg I/ml, 20 ml NaCl "chaser bolus", injection rate 4 ml/sec) was injected in an antecubital vein and detected by a series of low dose scans (120 kV, 30 mAs) performed at the height of the bifurcation of the pulmonary artery. The scans were initiated 10 sec. after contrast injection and were performed during breath hold at 2 sec. intervals for a duration of 30 sec. after injection begin.

The contrast enhanced MDCT scan was performed at the maximum gantry rotation time of 500 ms with a collimated slice with of  $4 \times 1$  mm resulting in an effective slice with of 1.25 mm. A spatial resolution of 9Lp/cm in the image



plane and 6Lp/cm in the longitudinal axis was achieved. 150 ml. of contrast agent (370 mg Iodine/ml) followed by a 30 ml. NaCl “chaser bolus” was injected at an rate of 4 ml/sec.. In order to achieve the best possible opacification of the coronary arteries, the scan was initiated with a delay after contrast injection according to the individual circulation delay time plus a correctional factor of 3 sec..

All CTA scans were performed at a set pitch of 0.375 which permitted continuous volume coverage in all 70 patients. If the chosen pitch is too great, the image stacks from subsequent cardiac cycles will not cover all z positions and gaps will occur in these image stacks (75,74), (Fig. 1).

Definition of pitch:  $P = \text{table travel per rotation/collimation of single slice}$

$$\text{Pitch} < (N - 1) T_{\text{rot}}/T_{\text{RR}}$$

- N : No. sections (slices)
- $T_{\text{RR}}$  : interval between subsequent R peaks
- $T_{\text{rot}}$  : full gantry rotation time

Fig. 1: Illustration of ECG-gated data acquisition with a 4-row scanner operating with continuous table feed and exposure. Image stacks from any given phase of the cardiac cycle can be reconstructed when the pitch is adapted to the patient heart rate (pitch is indicated by the level of incline of the intermittent lines). The phase of reconstruction ( $T_Q$ ) is defined in relation to the R-wave ( $T_{rew}$ ), (75).

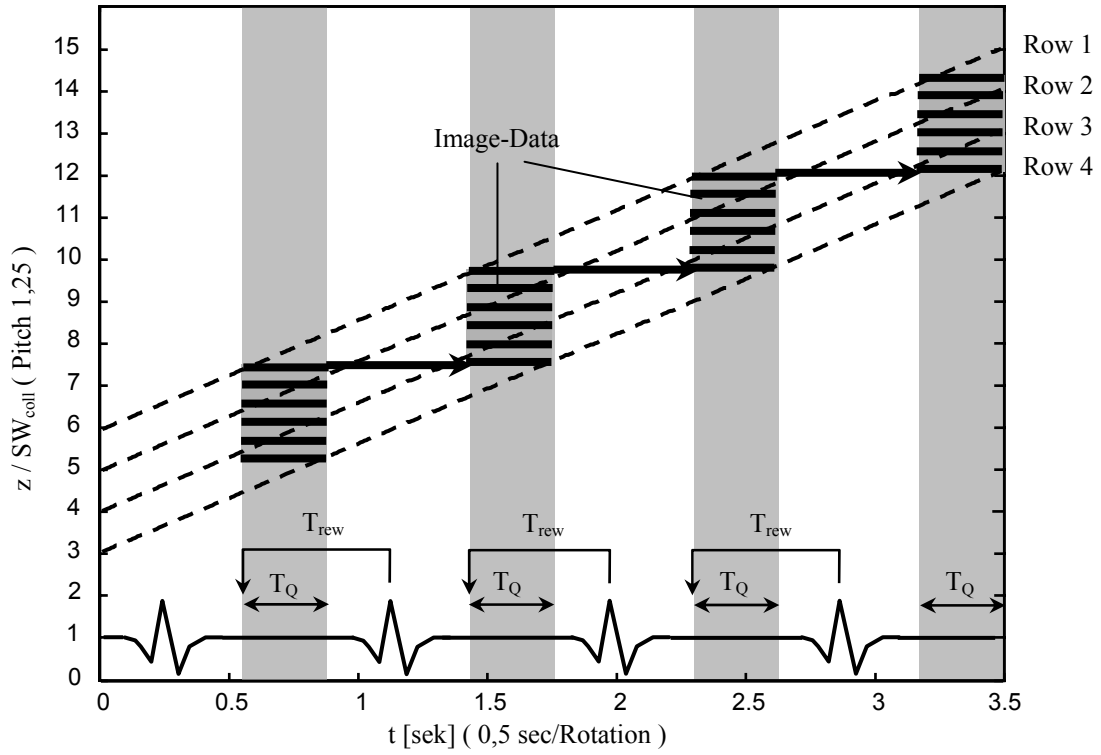


Fig. 2: Scan parameters for native and MDCT angiography study.

	<b>Native study</b>	<b>MDCT angiography</b>
Contrast agent	None	150 ml; 370 mg I/ml; 4 ml/sec
Collimation	4 x 2,5 mm	4 x 1 mm
Gantry rotation time	500 ms	500 ms
kV	140	140
mA	100	300
Slice with	3 mm	1,25 mm
Increment	1 mm	0,5 mm
Scan time	15 sec - 25 sec	22 sec - 49 sec

### 2.3. Post Processing and Image Reconstruction

CT angiography of the coronaries is not possible if the images can not be matched to the ECG of the patient. The method used in this study is known as retrospective ECG gating. With this technique the ECG of the patient is recorded simultaneously to the MDCT scan. Thereby, the spiral data can be matched to the cardiac cycle (ECG trace) and a phase for image reconstruction can be determined relative to the R wave.

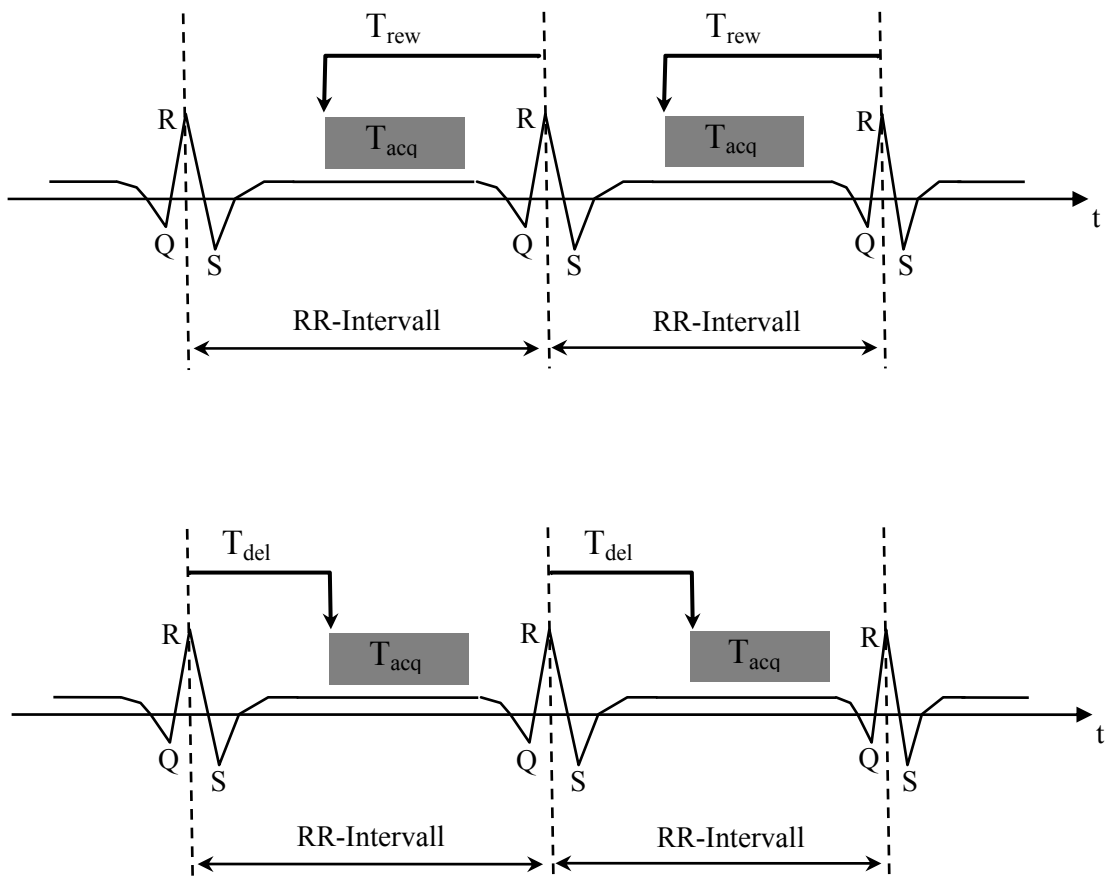
Two phase-selection strategies were used for image reconstruction:

With the relative-delay method the reconstruction is started at a certain fraction of the interval between R-waves (R-R interval). The actual delay time varies with the length of each cardiac cycle and is defined as a percentage of the R-R interval specified by the user.

When using the absolute-reverse-method the user defines a fixed time prior to the R wave at which the reconstruction interval is started. The reconstruction interval, therefore, is independent of the length of each cardiac cycle.

Both these approaches enable the user to obtain images from a consistent phase of subsequent heart cycles, thereby, avoiding misalignment of the images (76), (Fig 3).

Fig. 3: Illustration of retrospective gating. Top image shows absolute-reverse strategy:  $T_{rew}$  is constant prior to the next R wave. Bottom image shows relative-delay strategy: Delay time ( $T_{del}$ ) after the previous R wave is determined as a percentage of the R-R interval.(76)



## 2.4. Image Artefacts

To avoid artefacts, it is crucial to obtain images from the phase of the cardiac cycle in which the least amount of motion occurs. Due to the motion pattern of the heart and the different locations of the coronary segments, the coronary branches are not optimally visualized during one and the same interval of the cardiac cycle (4,46). To obtain the best set of images for each Coronary branch, images from different phases of the heart cycle must be reconstructed and evaluated. If the initial reconstructions did not yield satisfactory images, a test series of reconstructions at 40%, 50%, 60% and 70% of the R-R interval was performed in order to determine the optimal reconstruction phase for each coronary branch (37).

Stair-step artefacts are caused by inconsistent image alignment which occurs when the images from two subsequent heart rates are not obtained at the exact same phase of the cardiac cycle. The most common causes of this effect are cardiac arrhythmia and rapid heart rate. Stair-step artefacts also occur when the wrong phase of the cardiac cycle is chosen for image reconstruction.

Blurring artefacts are caused by motion within the image acquisition time.

Since both stair-step and blurring artefacts occurs with cardiac motion, a combination of both may be observed (32,40).

Applying a  $\beta$ -blocker prior to the scan will minimizing motion artefacts by slowing down the heart rate, thereby prolonging the diastole. In this study the individual medication of each patient was not altered and no pre scan  $\beta$ -blocker was given.

Fig. 4: Illustration of Stair-Step artefact: Effects of inconsistent image alignment.

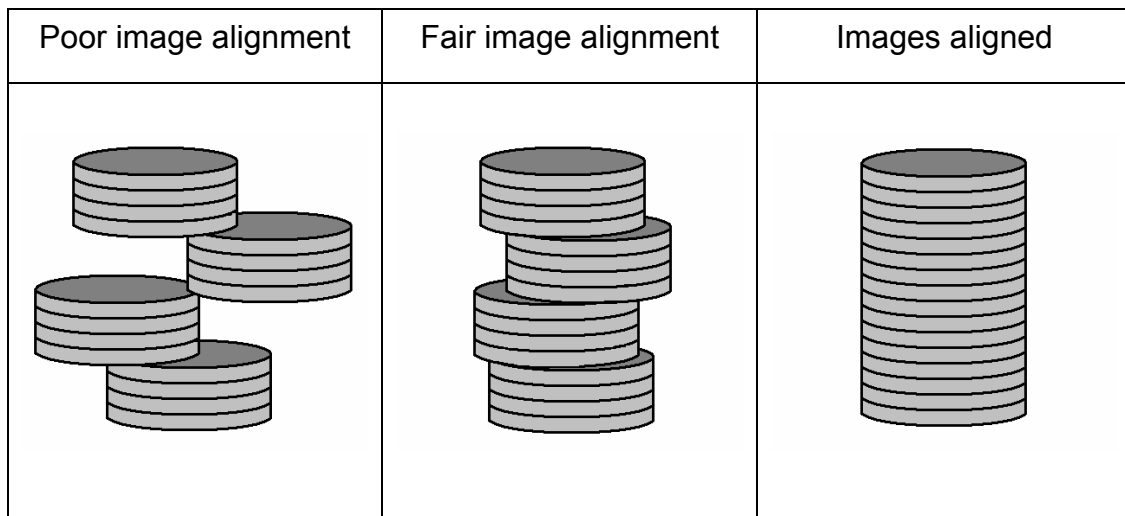


Fig. 5: Illustration of Image Blurring: Effect of cardiac motion within the image acquisition time.

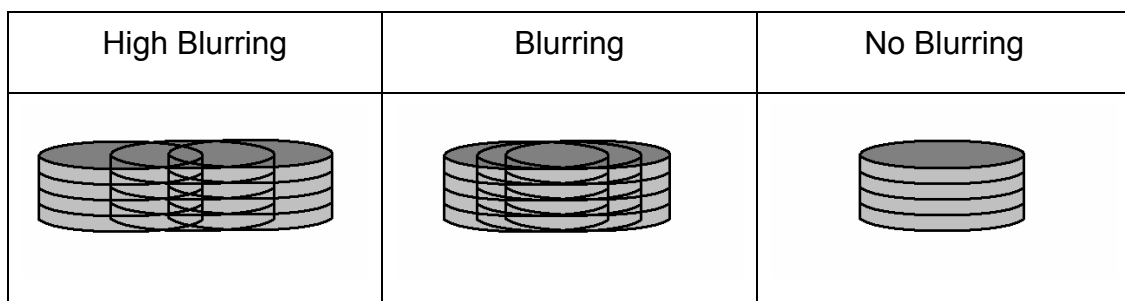
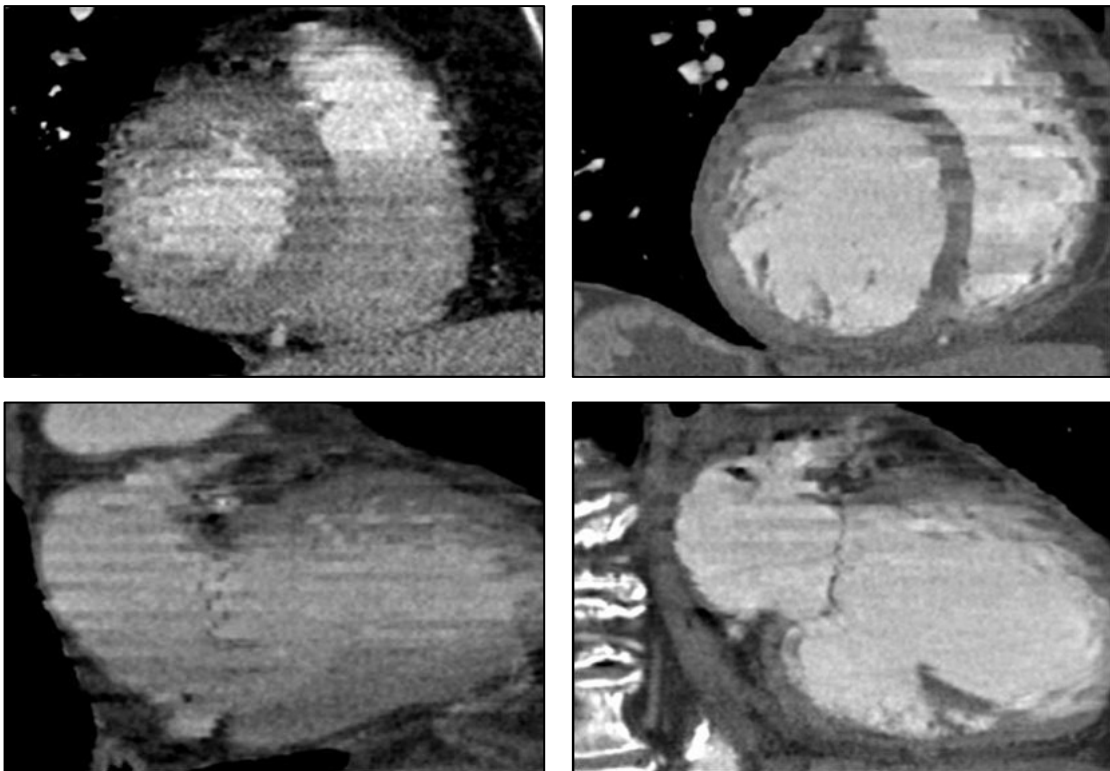


Fig. 6: Short axis- (top images) and long axis views (bottom images) of the heart, reconstructed from a four-row MDCT data set. The images demonstrate stair-step artefacts during systole (left images) and diastole (right images) of the cardiac cycle. Because of the rapid motion during systole, stair-step artefacts are fare more abundant during this cardiac phase.



As a rule, the temporal resolution in CT imaging is limited to  $\frac{1}{2}$  the gantry rotation time ( $t_{rot}/2$ ) since scan data from no less than  $180^\circ$  rotation is needed for the reconstruction of a complete image (33). A temporal resolution of  $500\text{ms}/2 = 250\text{ms}$ , however, is inadequate for cardiac imaging at high heart rates. To further reduce temporal resolution, prototype reconstruction software, which uses the adaptive cardio volume (ACV) reconstruction technique, was made available by Siemens Ag, Erlangen, Germany. This software achieves a reduction of the temporal resolution by combining scan data from two heart cycles into a single image when the heart rate exceeds a certain frequency (62 beats per min.). By using data from more than one cardiac cycle, the temporal resolution is no longer limited to half of the gantry rotation time ( $t_{rot}/2$ ), since less than  $180^\circ$  rotation per heart cycle is needed for image reconstruction. The limiting factor becomes the number (N) of consecutive cardiac cycles from which scan data is used and the temporal resolution is defined by the equation  $t_{rot}/2N$  (33). In this study, data from no more than 2 consecutive heart cycles were combined and the temporal resolution was limited to  $t_{rot}/2 \times 2 = 125\text{ms}$ .

## 2.5. Image Display

After the reconstruction of the axial images, the data volumes were visualized and evaluated on a 3D work station (Virtuoso®, Siemens, Forchheim, Germany) capable of creating Shaded-Surface-Displays, Maximum Intensity Projections and Volume Rendering. The location of stenosis was defined according to the definition of the American Heart Association and the detected stenoses were recorded on a semi quantitative scale (high grade stenosis:  $>70\%$  of vessel lumen, intermediate stenosis 50 - 70% of vessel lumen, wall irregularity:  $<50\%$  of vessel lumen), (Fig. 7). The reader was blind to the findings of the conventional coronary angiogram.



## 2.6. Ca-scoring

Calcium scoring was performed on a 3D Virtuoso® work station (Virtuoso®, Siemens, Forchheim, Germany). The process was semi automated, requiring a slice by slice analysis of the 3mm “scout” images in which the reader was required to assign detected calcification to a coronary artery or to discard it. The Calcium score was then generated automatically by the software, according to the algorithm introduced by Agatston et al (7).

The effect of coronary calcification was determined by dividing the patient population into two sub-groups with Agatston-scores above and below 100. The comparative statistical analysis to determine CTA performance for detection of coronary lesions was performed separately for each sub-group.

## 2.7. Conventional Angiography with Quantitative Coronary Analysis

All 70 patients underwent conventional coronary angiography 1 - 2 days after CTA examination. The procedure was performed according to the Judkins technique with which a catheter is introduced via the brachial or femoral artery into the ostium of each of the two coronary arteries. A contrast agent (Imeron®, 400 mg Iodine/ml, Altana Pharma, Konstanz) was injected and a series of images were recorded using a conventional X-ray generator and an image intensifier. The RCA was evaluated in 2 standard projections (LAO/RAO 45°) and the LCA in 6 Standard projections (RAO 15°, 35 -15°, 35 +15°, LAO 45 +15°, 60°, 90°). The initial evaluation was performed on sight by the attending physician.

In order to validate the results, the conventional Angiograms were additionally evaluated with the use of quantitative coronary analysis software (QCA, Philips Medical Systems, Eindhoven, Netherlands), by which the contour of each vessel lesion is automatically analysed and calibrated using the projection of the catheter as a standard measurement for calibration.

To facilitate the later comparison with the results of CTA, Each detected stenosis was classified according to the same system. (high grade stenosis:  $\geq$  70% of vessel lumen, intermediate stenosis 50 - 70% of vessel lumen, wall irregularity: <50% of vessel lumen).

## 2.8. Data Evaluation and Statistics

The analysis of the data is based on the comparison of each single coronary segment seen in CTA with conventional coronary angiography representing the gold standard. For this purpose each coronary segment is classified as either Positive = Stenosis or negative = no stenosis. The stenosed segments are divided into 3 categories according to the extent of lumen narrowing (high grade stenosis: >70% of vessel lumen, intermediate stenosis 50 - 70% of vessel lumen, wall irregularity: <50% of vessel lumen). Each coronary segment is thus categorized with both conventional- and CT-angiography, making it possible to define the CTA results for each segment as either true positive, false positive, true negative or false negative. Separate evaluations for high grade and intermediate stenoses can be performed. This classification of each coronary segment forms the basis for the descriptive statistical analysis of the data. Sensitivity, specificity, positive and negative predictive value of the CTA results compared to CCA can thus be determined.

Since a large number of distal segments cannot be adequately depicted with CTA, only the proximal segments 1, 2, 5, 6, 7 and 11 of the coronary tree are included in the data analysis presented in the results section of this thesis.

An analysis including the distal segments of the coronary tree leads to a false representation of CTA performance since a large number of segments must be omitted from such an analysis. The evaluation of CTA performance in distal coronary segments leaves room for much speculation and will be presented in the discussion at the end of this paper.

In order to demonstrate the influence of lesion size, coronary motion, heart rate, coronary calcification and lesion location within the coronary tree, different evaluations of the data were performed, accounting for these factors.

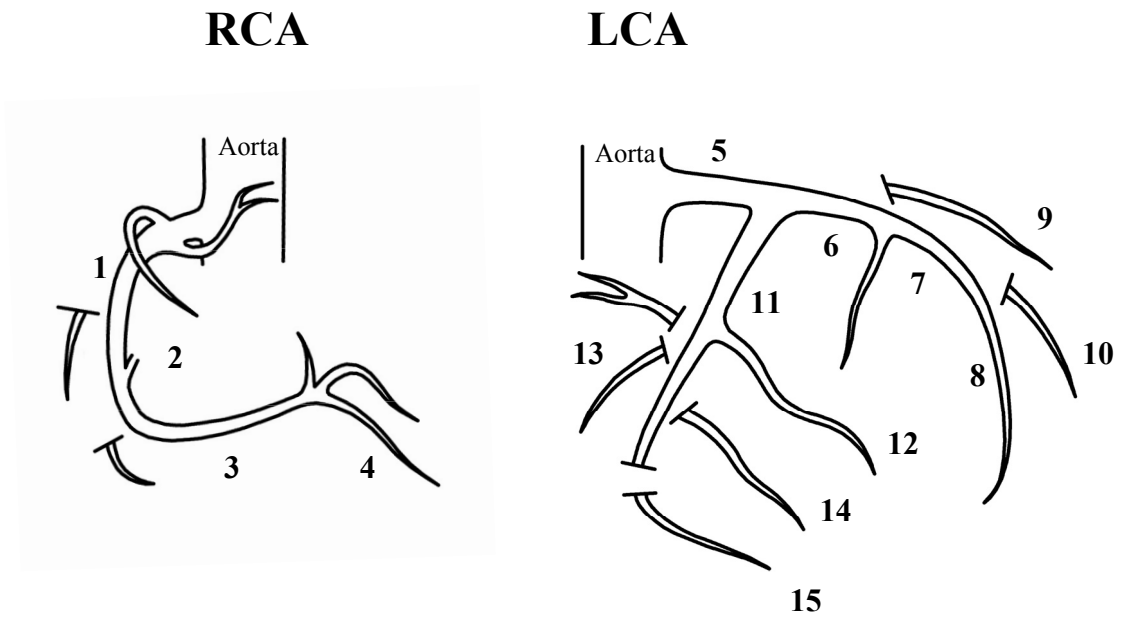
Separate statistical evaluations were performed for:

- Lesions > 70% and >50% of the coronary lumen
- Lesions within each of the separate coronary arteries (LAD, RCA and LCX)
- Studies performed at heart rates above and below 60 beats/min
- Studies with calcium scores above and below 100 Agatston

The influence of each factor can be determined by comparing the separate results of each analysis.

An additional evaluation was performed to determine the influence of iodinated contrast agent on heart rate. During the native and the contrast enhanced scan the EKG-trace of each patient was recorded. The individual heart rate of each patient was extracted from the recorded data and the heart rate within each one second intervals after scan begin was determined. Finally the mean heart rates of all patients during native and contrast enhanced scan could be compared at each one second interval after scan initiation. The extent of correlation between the mean patient heart rate before and after injection of contrast media is considered to be significant if the difference of the mean heart rates is smaller than the 95% confidence interval of the heart rates during the native scan.

Fig. 7: Diagrams illustrating the anatomy of the right coronary artery (lateral projection, segments 1 – 4) and left coronary artery (right anterior oblique projection, segments 5 -15). The segments are defined according to the American Heart Association (8).



## 3. Results

### 3.1. Study Population

The study population consisted of 13 female and 57 male patients between 33 and 76 years of age (mean 60). The mean heart rate was 63 beats per min. during the native MDCT scan (range 42 - 107) and 63 beats per min. during the contrast enhanced MDCT scan (range 43 - 92). The average calcium burden of the patients was found to be 330 agatston (range 0 - 3138).

The 70 CCA and 70 CTA exams were all performed successfully. The MDCT scan time varied according to scan volume and heart rate. The average scan time was 20 sec. (range 15 - 25) for the native, and 37 sec. (range 22 - 49) for contrast enhanced scan. All patients included in this study were able to hold their breath for the entire scan duration.

### 3.2. Detection of Coronary Lesions by CTA and CCA.

In the 70 Patients included in the study a total of 420 proximal coronary segments (1, 2, 5, 6, 7 and 11) were evaluated with CCA, of these segments 406 (96%) could be evaluated with CTA. The remaining 14 segments could not be evaluated due to poor image quality.

With CCA, The 420 coronary segments included in the study were found to contain a total number of 97 stenoses greater 50% of the vessel diameter, of these stenoses 70 (72%) were haemodynamic relevant ( $\geq 70\%$  of vessel lumen).

CTA was able to detect 86 (89%) of all stenoses, and 57 (81%) of the stenoses greater than 70% of vessel lumen (Fig. 8 and 9).

Of the 100 stenoses seen in CCA, 1(1%) was located in the LM, 41 (42%) in the RCA, 40 (41%) in the LAD and 15 (15%) in the LCX (Fig 10 - 12).

The statistical evaluation of the data to determine sensitivity, specificity, positive and negative predictive value for CTA detection of coronary lesions greater 50% of lumen diameter showed a sensitivity of 0.89 and a specificity of 0.90. Positive and negative predictive values were 0.73 and 0.96, respectively (Fig. 8).

Fig. 8: Sensitivity, specificity, positive and negative predictive value for MDCT detection of coronary stenoses greater than 50% diameter of vessel lumen.

		CCA	
		Pos.	Neg.
CTA	Pos.	True Pos. <b>86</b>	False Pos. <b>32</b>
	Neg.	False Neg. <b>11</b>	True Neg. <b>277</b>

n(Pat.) = 70  
 n(Seg.) = 406  
 n(Sten.) = 97

Sensitivity:	<b>0.89</b>
Specificity:	<b>0.90</b>
Pos. pred. Value:	<b>0.73</b>
Neg. pred. Value:	<b>0.96</b>

### 3.3. Influencing Factors for CTA Performance

A number of factors possess the potential to interfere with image quality, thereby influence coronary lesion detection by CTA. In order to demonstrate the influence of lesion size, coronary motion, heart rate and coronary calcification, different evaluations of the data were performed, accounting for these factors.

### 3.3.1. Lesion Size

When raising the threshold for stenosis from 50% to 70% of the vessel lumen, so that only haemodynamic relevant stenoses enter the evaluation, the sensitivity decreases from 0.89 to 0.81 while an increase of specificity from 0.90 to 0.93 is observed. Positive and negative predictive values remain practically unchanged (0.73 to 0.72 and 0.96 to 0.96 respectively), (Fig. 8 - 9).

Fig. 9: Sensitivity, specificity, positive and negative predictive value for MDCT detection of coronary stenoses greater than 70% diameter of vessel lumen.

		CCA	
		Pos.	Neg.
CTA	Pos.	True Pos. <b>57</b>	False Pos. <b>22</b>
	Neg.	False Neg. <b>13</b>	True Neg. <b>314</b>

n(Pat.)= 70  
 n(Seg.)= 406  
 n(Sten.)= 70

Sensitivity:	<b>0.81</b>
Specificity:	<b>0.93</b>
Pos. pred. Value:	<b>0.72</b>
Neg. pred. Value:	<b>0.96</b>

### *3.3.2. Lesion Location Within the Coronary Tree*

Because of the different motion pattern and velocity of each coronary branch during the cardiac cycle, more artifacts must be expected when evaluating those segments which move with greater velocity.

It has been shown that the RCA and the LCX are subjected to motion of greater velocity during the cardiac cycle than the LAD, and thus, more stair step and blurring artifacts are seen in the CT-Angiograms of these vessels (4,40). If coronary motion causes a reduction in image quality, we expect to see better results for detection of coronary stenoses in those branches which experience less motion during the cardiac cycle.

To determine the influence of lesion location within the coronary tree, separate evaluations of the data were performed for each of the three branches (RCA, LAD and LCX). The left main (segment 5) was excluded from this evaluation, since only one of the 70 examined segments was stenosed. This very low number of coronary lesions would result in an inaccurate evaluation.

The comparison of the statistical results for each separate coronary branch yields values for sensitivity of 0.95, 0.88 and 0.73 for the LAD, RCA and LCX, in the given order. A different order for the values of specificity (0.89 for the RCA, 0.86 for the LAD and 0.87 for the LCX) was seen. The results for positive and negative predictive value were 0.78 and 0.94 for the RCA, 0.73 and 0.98 for the LAD, 0.61 and 0.92 for the LCX (Fig 10 – 12).



Fig. 10: Sensitivity, specificity, positive and negative predictive value for MDCT detection of coronary stenoses greater than 50% diameter of vessel lumen. Evaluation of the LAD (Segments 6 and 7).

		CCA	
		Pos.	Neg.
CTA	Pos.	True Pos. <b>38</b>	False Pos. <b>14</b>
	Neg.	False Neg. <b>2</b>	True Neg. <b>83</b>

n(Pat.)= 70  
 n(Seg.)= 137  
 n(Sten.)= 40

Sensitivity:	<b>0.95</b>
Specificity:	<b>0.86</b>
Pos. pred. Value:	<b>0.73</b>
Neg. pred. Value:	<b>0.98</b>

Fig. 11: Sensitivity, specificity, positive and negative predictive value for MDCT detection of coronary stenoses greater than 50% diameter of vessel lumen. Evaluation of the RCA (Segments 1 and 2).

		CCA	
		Pos.	Neg.
CTA	Pos.	True Pos. <b>36</b>	False Pos. <b>10</b>
	Neg.	False Neg. <b>5</b>	True Neg. <b>81</b>

n(Pat.)= 70  
 n(Seg.)= 132  
 n(Sten.)= 41

Sensitivity:	<b>0.88</b>
Specificity:	<b>0.89</b>
Pos. pred. Value:	<b>0.78</b>
Neg. pred. Value:	<b>0.94</b>

Fig. 12: Sensitivity, specificity, positive and negative predictive value for MDCT detection of coronary stenoses greater than 50% diameter of vessel lumen.

Evaluation of the LCX (Segment 11)

		CCA	
		Pos.	Neg.
CTA	Pos.	True Pos. <b>11</b>	False Pos. <b>7</b>
	Neg.	False Neg. <b>4</b>	True Neg. <b>45</b>

n(Pat.)= 70  
 n(Seg.)= 67  
 n(Sten.)= 15

Sensitivity:	<b>0.73</b>
Specificity:	<b>0.87</b>
Pos. pred. Value:	<b>0.61</b>
Neg. pred. Value:	<b>0.92</b>

### 3.3.3. Heart Rate

A major challenge for coronary CTA is the occurrence of motion artifacts resulting from the rapid motion of the coronary vessels during the cardiac cycle. Only data from the diastole part of the cardiac cycle should be used for image reconstruction in order to avoid stair step and blurring artifacts that hinder the evaluation. In patients with high heart rates the diastole becomes shorter, resulting in a narrower temporal window for image reconstruction, thus leading to more motion artifacts (39,67,72,90).

In order to determine how heart rate influenced the detection of coronary lesions in the patient group, separate evaluations were performed for patients with heart rates above and below 60 beats per minute (Fig 13 and 14).

In the patient group with heart rates below 60 beats per minute, higher values for sensitivity (0.89) and specificity (0.92) were observed, compared to sensitivity (0.88) and specificity (0.88) of the patient group with heart rates above 60 beats per minute. The same pattern was seen for the positive predictive value, which was 0.82 for the group with heart rates below, and 0.63 for that with heart rates above 60 beats per minute. The negative predictive value of 0.95 in the group with high heart rates was slightly lower compared to 0.97 in the group with lower heart rates (Fig 13 and 14).

Fig. 13: Sensitivity, specificity, positive and negative predictive value for MDCT detection of coronary stenoses > 50% diameter of vessel lumen, in a group of patients with heart rates below 60 beats per minute.

		CCA	
		Pos.	Neg.
CTA	Pos.	True Pos. <b>51</b>	False Pos. <b>11</b>
	Neg.	False Neg. <b>6</b>	True Neg. <b>126</b>

n(Pat.)= 33  
 n(Seg.)= 194  
 n(Sten.)= 57

Sensitivity:	<b>0.89</b>
Specificity:	<b>0.92</b>
Pos. pred. Value:	<b>0.82</b>
Neg. pred. Value:	<b>0.95</b>

Fig. 14: Sensitivity, specificity, positive and negative predictive value for MDCT detection of coronary stenoses > 50% diameter of vessel lumen, in a group of patients with heart rates above 60 beats per minute.

		CCA	
		Pos.	Neg.
CTA	Pos.	True Pos. <b>35</b>	False Pos. <b>21</b>
	Neg.	False Neg. <b>5</b>	True Neg. <b>151</b>

n(Pat.)= 37  
 n(Seg.)= 212  
 n(Sten.)= 40

Sensitivity:	<b>0.88</b>
Specificity:	<b>0.88</b>
Pos. pred. Value:	<b>0.63</b>
Neg. pred. Value:	<b>0.97</b>

### *3.3.4. Coronary Calcium*

The high density of calcifications within coronary vessels makes calcium well visible in CT, but also may result in misinterpretation caused by artifacts.

The Effect of coronary calcification on CTA detection of coronary stenoses was determined by performing separate evaluations of the data for patients with agatston scores above and below 100 Agatston (Fig. 15 and 16).

When comparing the statistical results of coronary CTA of patients with calcium scores above and below 100, an increase in sensitivity from 0.84 for patients with scores below 100 to 0.90 for those patients with scores above 100 can be observed. The specificity rose slightly from 0.89 to 0.91.

The positive predictive value for the patient group with calcium scores below 100 was very low (0.53) compared to the patient group with scores above 100 (0.83). The negative predictive value shows a slight decrease from 0.97 for patients with scores below, to 0.95 for those with scores above 100 (Fig 15 and 16).

Fig. 15: Sensitivity, specificity, positive and negative predictive value for MDCT detection of coronary stenoses > 50% of vessel lumen diameter in a group of patients with Ca. Scores below 100 Agatston.

		CCA	
		Pos.	Neg.
CTA	Pos.	True Pos. <b>21</b>	False Pos. <b>19</b>
	Neg.	False Neg. <b>4</b>	True Neg. <b>147</b>

n(Pat.)= 33  
 n(Seg.)= 191  
 n(Sten.)= 25

Sensitivity:	<b>0.84</b>
Specificity:	<b>0.89</b>
Pos. pred. Value:	<b>0.53</b>
Neg. pred. Value:	<b>0.97</b>

Fig. 16: Sensitivity, specificity, positive and negative predictive value for MDCT detection of coronary stenoses > 50% of vessel lumen diameter in a group of patients with Ca. Scores above 100 Agatston.

		CCA	
		Pos.	Neg.
CTA	Pos.	True Pos. <b>65</b>	False Pos. <b>13</b>
	Neg.	False Neg. <b>7</b>	True Neg. <b>130</b>

n(Pat.)= 37  
 n(Seg.)= 215  
 n(Sten.)= 72

Sensitivity:	<b>0.90</b>
Specificity:	<b>0.91</b>
Pos. pred. Value:	<b>0.83</b>
Neg. pred. Value:	<b>0.95</b>

### 3.3.5. Summery of Results

Fig 17: Evaluation of all Stenoses with a threshold of 50% and 70% diameter of the coronary lumen. (Coronary segments 1, 2, 5, 6, 7 and 11)

	Sensitivity	Specificity	Pos. Predictive Value	Neg. Predictive Value
All Stenoses above 50%	0.89	0.90	0.73	0.96
All Stenoses above 70%	0.81	0.93	0.72	0.96

Fig 18: Separate evaluation of each coronary branch. (Threshold for Stenosis: 50% of vessel lumen diameter), (Coronary segments 1, 2, 5, 6, 7 and 11)

	Sensitivity	Specificity	Pos. Predictive Value	Neg. Predictive Value
Left Main (Seg. 5)	1.00	0.99	0.50	1.00
LAD (Seg. 6 and 7)	0.95	0.86	0.73	0.98
LCX (Seg. 11)	0.73	0.87	0.61	0.92
RCA (Seg. 1 and 2)	0.88	0.89	0.78	0.94

Fig 19: Separate Evaluation for Patients with heart rates above and below 60 beats per min. (Threshold for Stenosis: 50% of vessel lumen diameter), (Coronary segments 1, 2, 5, 6, 7 and 11)

	Sensitivity	Specificity	Pos. Predictive Value	Neg. Predictive Value
Heart rate $\leq$ 60/min	0.89	0.94	0.89	0.94
Heart rate $>$ 60/min	0.88	0.88	0.59	0.97

Fig 20: Separate evaluations for patients with coronary calcium burden above and below 100 Agatston. (Threshold for Stenosis: 50% of vessel diameter), (Coronary segments 1, 2, 5, 6, 7 and 11)

	Sensitivity	Specificity	Pos. Predictive Value	Neg. Predictive Value
Ca.-Score $\leq$ 100 Agatston	0.84	0.89	0.53	0.97
Ca.-Score $>$ 100 Agatston	0.90	0.91	0.83	0.95



### 3.4. Influence of Contrast Media on Patient Heart Rate.

The intravenous application of iodinated contrast media may cause variations in patient heart rate (61). Since a slow and rhythmic heart rate is a key condition for high quality coronary CTA studies, it is important that the application of contrast media does not cause a severe increase in patient heart rate during the CTA examination (39,90).

In order to determine if the application of contrast media significantly affected the mean patient heart rate during the CTA examination, the ECG traces of both the native and the CTA scan were analyzed. The mean heart rates of the 70 patients were determined at one second intervals after scan begin (Fig 21 and 22). Thereby, a direct comparison of the values could be performed (Fig 23). The average scan time was 20 sec. for the native, and 37 sec. for the CTA scan, limiting the comparison of heart rate to the first 20 seconds. The initial decrease in heart rate followed by a steady increase is a physiological reaction during breath hold, caused by vagal nerve activity (63).

Fig. 21: Maximum, minimum and mean heart rate +/- one standard deviation in 70 patients during native MDCT scan, plotted at 1sec. intervals.

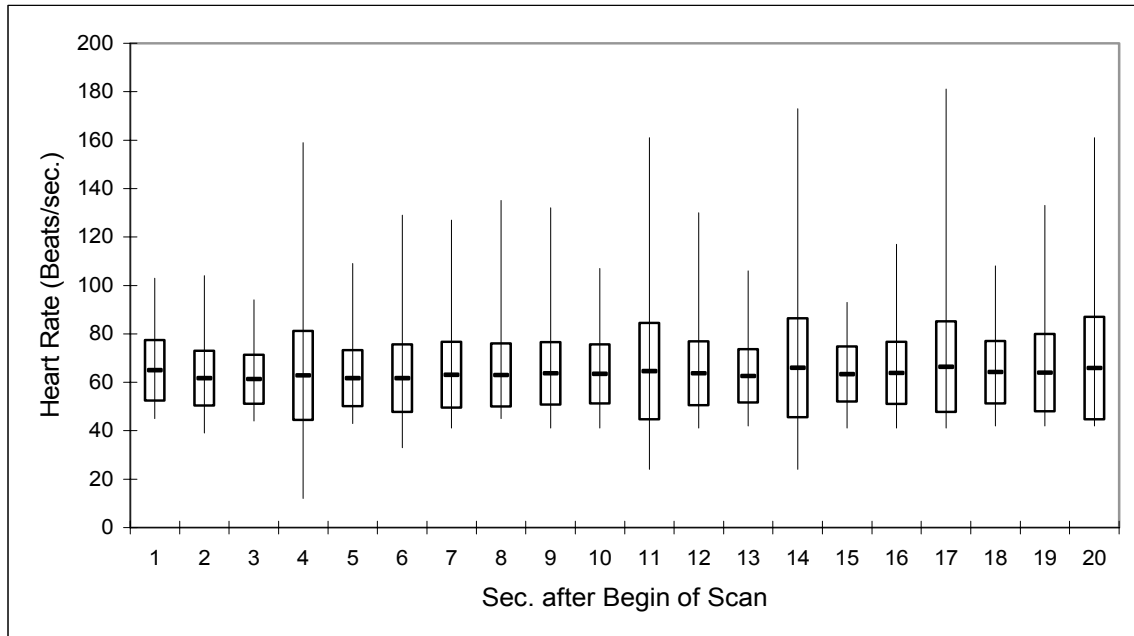


Fig. 22: Maximum, minimum and mean heart rate +/- one standard deviation in 70 patients during contrast enhanced MDCT scan, plotted at 1sec. intervals.

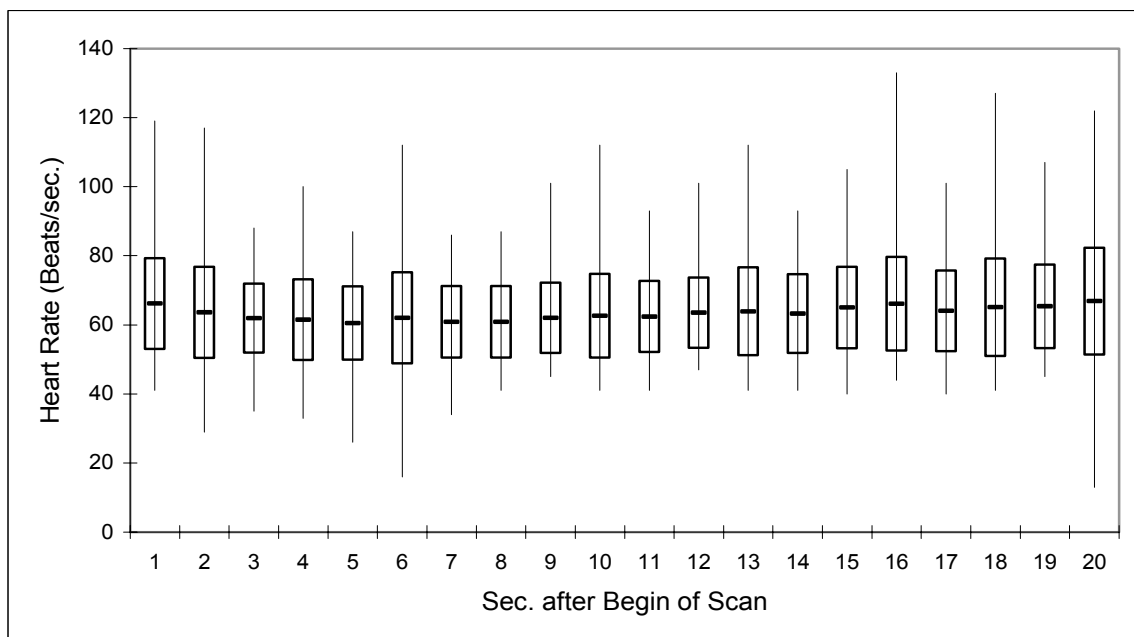
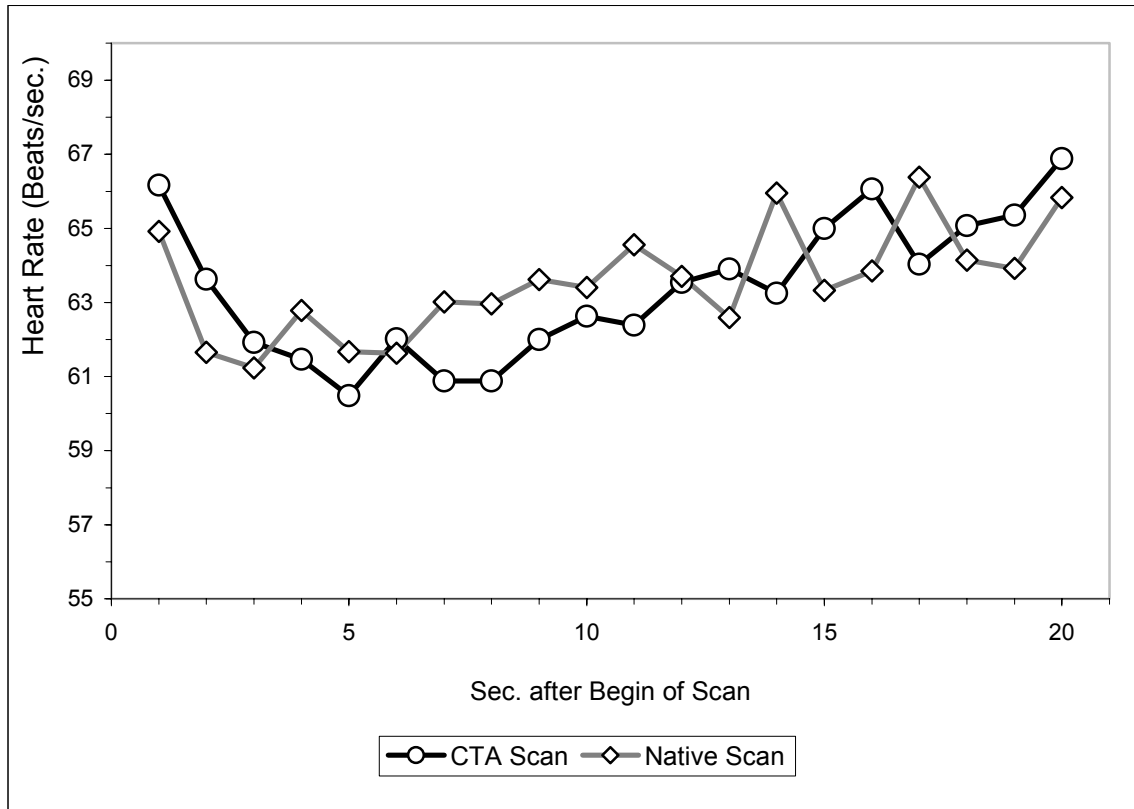


Fig. 23: Mean heart rate of 70 patients during native and contrast enhanced CT scan, plotted at 1 sec. intervals for 20 sec. after scan begin.



When observing the changes in heart rate during the native and contrast enhanced scan, it becomes evident that there is little or no difference between the two graphs (Fig. 23).

The statistical proof of correlation between the two graphs is obtained by calculating the difference of the mean heart rates in the 70 patients during the native and contrast enhanced scan. The obtained figure is then compared to the 95% confidence interval of the heart rate values of the native scan. If the difference of heart rate is smaller than the 95% confidence interval, the probability of a significant difference between the two set of values is less than 5% ( $p < 0.05$ ) (36,42,44,66).

The following chart lists the difference in mean heart rate between the two scans and the 95% confidence interval of the native scan. The values have been calculated for each one second interval after scan initiation. Since the difference of heart rate is consistently smaller than the 95% confidence interval, there is no significant difference between the measured heart rates during native and contrast enhanced scan (9).

Fig 24: Difference in mean heart rate in 70 patients during native and contrast enhanced scan (middle column). 95% confidence interval of the heart rate values for the native scan (right column). Values calculated at 1 sec. interval after scan begin. The difference of heart rate between the two scans is continuously lower than the 95% confidence interval, suggesting a high level of correlation.

Sec. after begin of scan	Difference of heart rate between native and contrast enhanced scan	95% confidence interval of heart rates during native scan
1	1.25	2.94
2	1.97	2.67
3	0.69	2.37
4	1.32	4.33
5	1.19	2.71
6	0.39	3.28
7	2.14	3.19
8	2.09	3.06
9	1.62	3.04
10	0.77	2.87
11	2.17	4.67
12	0.16	3.11
13	1.31	2.60
14	2.71	4.80
15	1.67	2.68
16	2.21	3.02
17	2.35	4.38
18	0.93	3.04
19	1.44	3.77
20	1.05	4.97

### 3.5. Image Examples

Fig 25: Three dimensional volume rendered Images of a four-row MDCT data set showing the LM, LAD (a) and LCX (b) on the surface of the heart (b). Note the opacification of the venous structures in image b (arrow).

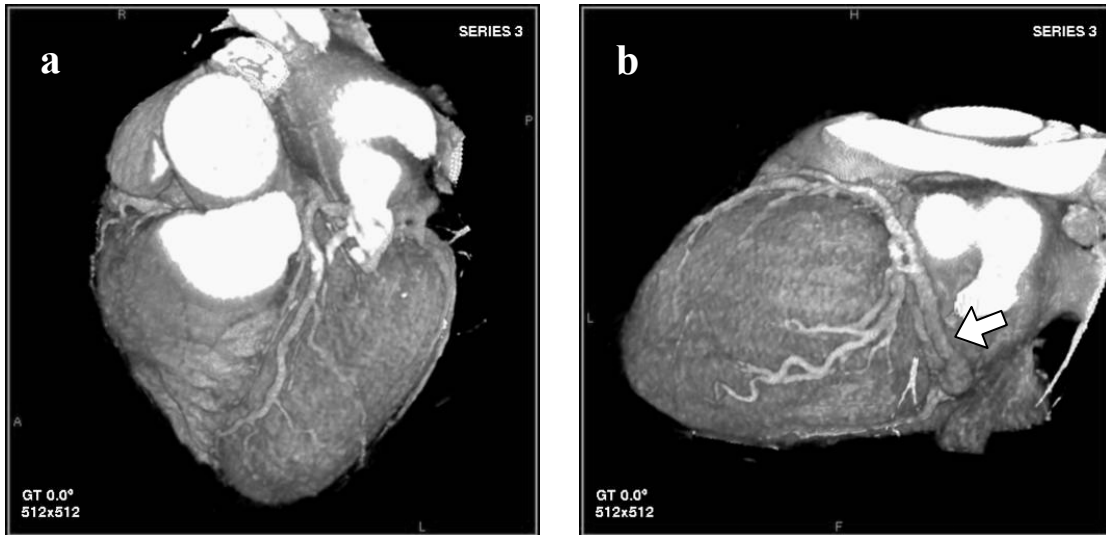
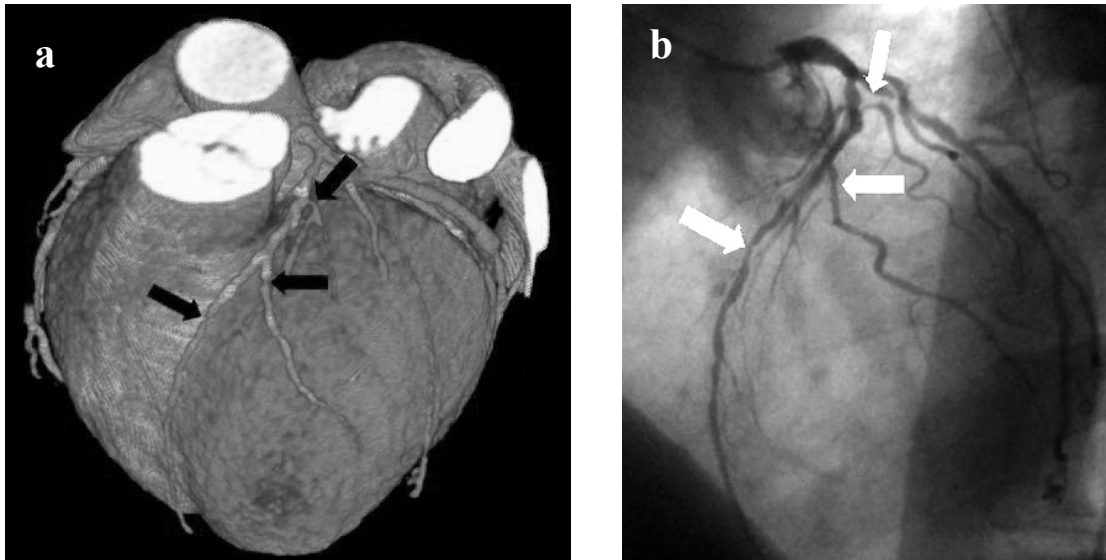


Fig 26: Volume rendered Images of a four-row MDCT data set showing the heart and the proximal (a) and distal (b) RCA. The distal branches of the RCA are depicted clearly (arrows).



Fig 27: Comparison of conventional invasive coronary angiography (b) and contrast enhanced four-detector row MDCT angiography (a) in one patient. The images are projected in the left anterior oblique (LAO) view. Both images show luminal narrowing of the LAD and the first and second diagonal branch (arrows).



## 4. Discussion

### 4.1. Limitations of CTA as a Diagnostic Tool for CAD

The rapid motion of the heart and the relatively small size of the coronary arteries account for the major difficulties associated with coronary angiography. MDCT offers high spatial and temporal resolution, and thereby meets the basic requirements for adequate depiction of the coronary vessels. This study shows a sensitivity of 0.89 and a specificity of 0.90 for stenoses greater than 50% of the lumen in proximal coronary segments, suggesting a high potential for the detection of coronary lesions. Adequate evaluation of the distal coronary segments, however, was not possible since only 59% of these segments were probably depicted with CTA. This fact reflects the necessity of even greater temporal and spatial resolution in MDCT angiography.

General disadvantages of coronary CTA include intravenous contrast media application and radiation exposure to the patient. The most severe complications associated with contrast media application are renal failure and anaphylactic reactions. Since iodinated contrast media is applied during both CTA and CCA, the adverse effects do not distinguish the two modalities from each other. Renal failure after application of iodinated contrast media is very rare in patients with good renal function and is usually reversible. Anaphylactic reactions can be very severe demanding immediate intensive care treatment, they occur within minutes of contrast media application. Anaphylactic shock, being the most severe reaction, may usually be avoided if symptoms are treated appropriately (30,62,64). Minor reactions to iodinated contrast media may occur up to several days after application. The most common of these late reactions are skin rash, nausea and headaches. Usually these manifestations require no medical treatment (103).

Coronary CTA is burdened with a relatively high radiation exposure to the patient. Studies have shown values of up to 11mSv for a single exam including native and contrast enhanced scan. These values are slightly higher than the average radiation dose of CCA exams (12,45). Radiation exposure is especially problematic if CTA is to be applied as a screening method for CAD in young patients in which the potentially carcinogenic effect is more severe. This disadvantage of CTA limits its potential as a widely applicable diagnostic tool.

## 4.2. Interfering Factors in Coronary CTA

### *4.2.1. Heart Rate*

In order to avoid motion artifacts, only minimal cardiac motion within the image acquisition time is tolerable. With a given image acquisition time of 250ms, the optimal window for image reconstruction within the diastole of the cardiac cycle is very narrow even at low heart rates (72,101). As heart rates increase, the systole phase of the cardiac cycle remains virtually unchanged while the diastole becomes shorter (25). This results in an even narrower acquisition window for image reconstruction and motion free reconstruction become virtually impossible. Each branch of the coronary tree has a different pattern of motion and consequently the optimal acquisition window varies for each branch and even for each coronary segment (4). Determining the best time for image reconstruction for each coronary branch is best achieved by performing a test series of reconstructions at different phases of the cardiac cycle and evaluating the different reconstruction series for each coronary branch (37,59,90). This procedure can be performed relatively quickly, due to technical developments allowing very short image reconstruction times (59).



A different approach to the problem of cardiac motion is to shorten the data-acquisition time. It is not possible to reduce the total time needed to acquire the data for a complete image, since the maximum gantry rotation time is limited, and a certain degree of gantry rotation is required for complete data acquisition. An approach has been made to combine the data of 2 subsequent cardiac cycles into one image, thereby reducing the temporal resolution by half. With a gantry rotation time of 0.5 sec., a reduction from 250ms to 125ms can be achieved. The drawback to this method is that the motion of the heart within the two given cardiac cycles must be identical for the data to match perfectly. This makes the approach very sensitive to any kind of variations in cardiac rhythm (76).

By choosing the right interval for image reconstruction within the cardiac cycle and applying dedicated spiral algorithms, motion artifacts can be reduced significantly (76).

Despite the attempts to minimize the effects of cardiac motion, high heart rates still do affect the outcome of coronary CTA. This becomes evident when observing the number of coronary segments that could not be adequately depicted due to poor image quality. The number of such segments is greater in studies performed at high heart rates. In the sub-group of patients with heart rates  $\leq 60$  beats/min (n=33), 14% of all coronary segments could not be adequately depicted with CTA. This number increases to 23% in the sub-group of patients (n=37) with heart rates above 60 beats/min.

The effect of increased heart rate is not as clearly reflected in the statistical evaluation of CTA performance in patients with heart rates above and below 60 beats per min.. CTA showed slightly higher values for sensitivity and specificity (0.89 and 0.92) for patients with heart rates below 60/min, compared to values of 0.88 and 0.88 for patients with higher heart rates.

These statistical values show such slight variation because only segments of good image quality were evaluated. All segments containing significant artifacts and all distal segments were excluded from the evaluation.

#### *4.2.2. Lesion Size*

It seems logical that larger coronary lesions are more easily detected in CTA than smaller ones. To determine the influence of this factor, a separate statistical evaluation including only stenoses greater than 70% of the vessel lumen was performed and compared to the evaluation including all stenoses (lumen narrowing > 50% diameter).

The decrease of sensitivity for detection of larger stenoses from 0.81 to 0.89 is initially surprising, since a greater sensitivity for larger lesions would be expected. The explanation for the, seemingly, lower detection rate of high grade stenoses is found in the underestimation of stenoses by CTA. Since the threshold for high grade stenoses was set at 70%, all high grade stenoses that were estimated to be below 70% with CTA were counted a false negative, accounting for the decrease of sensitivity.

The increase of specificity for high grade stenoses from 0.89 to 0.93 reflects the decrease of false positive segments. To understand this phenomenon, one must consider what causes a segment to be read as false positive. If the CTA image of a coronary segment contains artifacts or is simply of poor quality, the reader may believe to see a stenosis where there is none, thereby, creating a false positive result. The higher specificity observed for high grade stenoses reflects the lower number of false positive segments in this group. It can be concluded that most false positive findings were read as low grade stenoses.

#### *4.2.3. Lesion Location Within the Coronary Tree*

When analyzing the results of coronary CTA for each coronary branch separately, differences in outcome become evident. A number of factors can be held responsible for this phenomenon. Naturally, the size of the vessel contributes to the clear depiction in angiography, but vessel size alone is not the sole contributing factor (3,31).

The velocity and the pattern of motion of each coronary segment are responsible for motion artifacts and hinder the clear depiction of the vessels. Each segment of the coronary tree has a different motion pattern during the cardiac cycle, depending on the location of the vessel. Because of their position within the coronary groove, the RCA and LCX are subjected to more rapid motion during diastole than the LAD. This is caused mainly by atrial contraction during end diastole (2). Recent studies have shown that performance of EBCT and MDCT angiography is reduced by coronary motion, and that this factor is most evident in those coronary segments in which velocity of motion is greatest, namely the LCX and the RCA (3,4,31,40,59,71,86,101).

Since rapid coronary motion causes a reduction of image quality, we expect to see better results for detection of coronary stenoses in those branches which experience less motion during diastole. The separate evaluation of the data for each coronary branch yielded the highest sensitivity (0.95) for detection of coronary lesions within the LAD compared to the RCA and LCX with values of sensitivity of 0.88 and 0.73, respectively. This result is in accordance with the fact that the LAD experiences less rapid motion than the RCA and the LCX during the diastole phase of the cardiac cycle.

Only slight variations of specificity were observed between the three coronary branches, suggesting that the different motion patterns do not induce a large difference in false positive findings.

#### *4.2.4. Coronary Calcium*

Calcification of the coronary vessels is a common phenomenon frequently observed in patients with coronary heart disease (16,97). Although extensive coronary calcification indicates a high plaque burden, it does not necessarily coincide with coronary stenosis (19). It has been shown that presence of calcium within a coronary plaque is a sign of plaque remodeling which indicates coronary disease progression, but does not make the plaque more likely to rupture, causing an acute coronary event (16,18).

There is much controversy on the subject of coronary calcium serving as a predictor of future coronary events (49,57,91,93). While there is no question that coronary calcium is an entity of coronary heart disease, its role as a risk factor has not been firmly established. This, in part, is due to the inconsistency of the ca-score itself, which has been shown to have a rather high interscan variability and is dependent of factors such as body mass index, tube current and scoring method (5,47,60,92,94,98,102).

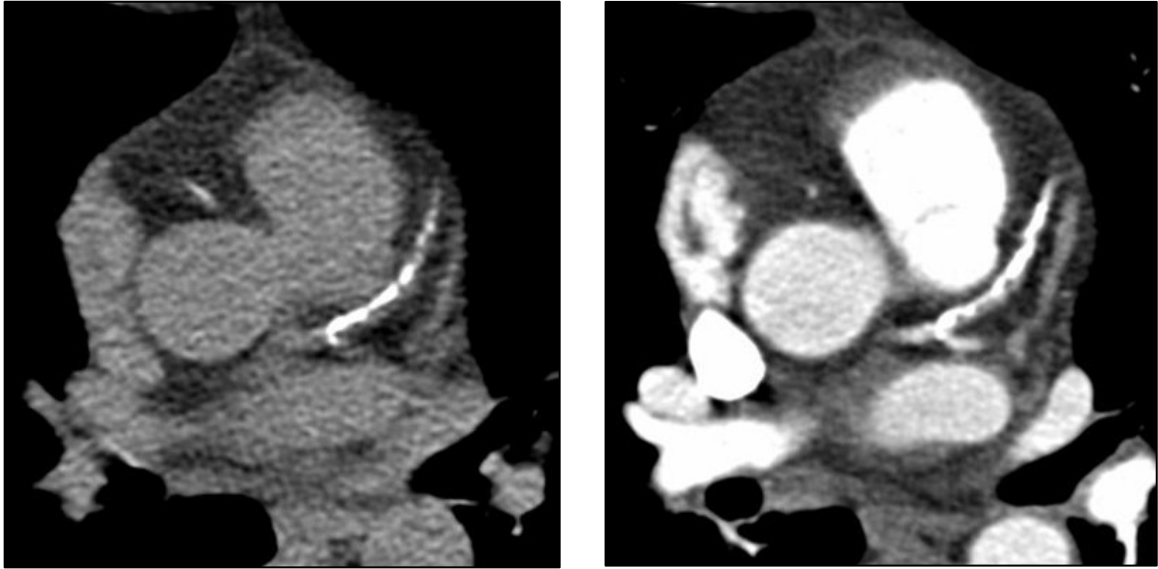
Coronary calcification introduces a number of challenges in coronary CTA. Vascular calcifications can cause blooming artifacts, making the plaque appear larger than it actually is (24). In CTA this may be falsely interpreted as stenosis or obliteration of the vascular lumen.

If the calcifications within a coronary vessel are of a similar density to the contrast enhanced lumen of this vessel, the calcified plaque may be mistaken for the actual vessel lumen. Vessels with extensive Calcifications may thus be falsely interpreted as patent. This phenomenon may be avoided by adjusting the window levels of the work station accordingly. Considering the pitfalls mentioned above, CTA exams showing coronary calcification must be read with caution.

An interesting observation can be made when comparing the separate evaluations for patients with high and low calcium burdens. One might expect that the artifacts caused by the calcifications would result in a lower sensitivity for coronary lesions, but there is a 5% increase of sensitivity in the group of patients with high calcium scores. A possible explanation for this result is that the calcium within the plaque draws the attention of the reader, resulting in a higher sensitivity for calcified lesions.

The dramatic decrease of positive predictive value (30%) in patients with high calcium scores is not surprising. It is caused by the overestimation of the calcified lesions, resulting in a very high number of false positive findings. This effect may be contributed to blooming artifacts caused by the high density of these lesions.

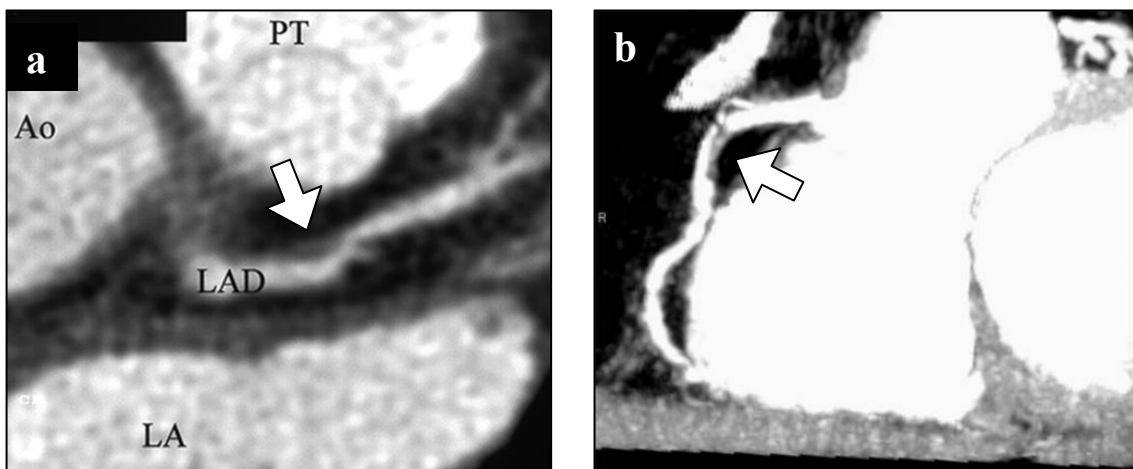
Fig. 30: Axial CT images from a contrast enhanced multi-row CT coronary angiography study showing calcifications of the LAD before (left image) and after (right image) application of contrast media. Assessment of the vessel lumen is hindered by the extensive vascular calcifications.



### 4.3. Soft Plaque

Soft plaques are coronary lesions that show no calcification and contain a lipid core covered by a thin fibrous cap. These lesions are less stable than calcified plaque and are more likely to rupture causing an acute coronary event (20,48,69,100). Soft plaques cannot be differentiated from other coronary lesions with CCA since only the vessel lumen and not the tissue of the lesion itself is depicted with this modality. Intravascular ultrasound may be performed during CCA in order to determine plaque morphology, but is an expensive procedure which is not performed on a standard basis (88). Ideally, soft plaques may be identified with CTA since coronary calcium is evident in CT angiograms (58,89). The potential of assessing plaque morphology is a strong advantage of CTA, but the small size of coronary lesions and the rapid cardiac motion demand an increase in spatial and temporal resolution for the reliable depiction of plaque morphology.

Fig. 31. Contrast enhanced multi-row CT coronary angiography studies showing soft plaques (arrows). (a) Multi-planer reformat showing soft plaque in the proximal LAD. (b) Thin slice MIP (Maximum Intensity Projection) showing a soft plaque in the proximal RCA.



#### 4.4. Influence of Contrast Media on Patient Heart Rate.

A number of studies have succeeded in showing how rapid cardiac motion challenges the outcome of coronary CTA, emphasizing the importance of slow and steady patient heart rate for consistent CTA performance (39,59,67,72,90). The application of intravenous contrast media may cause undesirable variations in patient heart rate, jeopardizing the outcome of the study (61).

An analysis of patient heart rates during the native scan and the contrast enhanced CTA scan was performed to determine if the application of contrast media caused significant change in heart rate. It could be shown, that no significant variation occurred.

This however, does not mean that the heart rates of patients undergoing coronary CTA remains steady during the scan. The observed variations are not caused by contrast media, but by vagal nerve activation which occurs during breath hold (63). These variations are observed during both the native and the contrast enhanced scan.

A clear drawback to the evaluation of the heart rate development during the native and the contrast enhanced scan is the limited time span of the ECG acquisition. Since the native scan is performed with a wider collimation than the contrast enhanced scan, it is considerably shorter, showing an average scan time of 20 sec. compared to 37 sec.. For this reason the comparison of the heart rate during the two scans was limited to the first 20 sec. after scan begin. A longer time range would be desirable in order to determine any effects that the application of contrast media might cause later than 20 sec. after application.



#### 4.5. Limitation of the Study

The results presented to this point have been limited to the evaluation of the proximal segments of the coronary tree. 96% of these segments could be evaluated with CTA. The statistical analysis of the data presents a true image of the collected data, since only 4% of the coronary segments had to be omitted from the evaluation due to poor quality of the CTA exam.

The distal segments are excluded from the evaluation presented in the results section of this study because a large number (41%) of these segments could not be adequately visualized with CTA. An evaluation of all segments depicted with both CCA and CTA presents a false image of CTA performance, since it does not reflect the fact that 19% of the total number of segments are excluded from the analysis due to poor image quality. The results of this analysis are presented in Fig. 28.

An evaluation including all 769 coronary segments is not permissible since the 143 segments that could not be adequately depicted in CTA cannot be classified as stenosed (positive) or normal (negative). This classification is the basis of the statistical analysis.

In order to allow the classification of the 146 remaining segments, the assumption can be made that all segments not adequately depicted in CTA are classified as normal (negative). In this case, every single segment can be categorized as true positive, false positive, true negative or false negative and all 769 segments may enter the evaluation. The results of this analysis are presented in Fig. 29 and show a relatively low value for sensitivity of 0.73. It must be emphasized, that this evaluation of the data is based on assumption and does not present a true image of the collected data. The resulting values however, may be closer to the truth, since they are not biased by omitting the coronary segments that could not be depicted with CTA.

Fig. 28. Sensitivity, specificity, positive and negative predictive value for MDCT detection of coronary stenoses greater than 50% diameter of vessel lumen in all coronary segments seen with both CTA and CCA.

		CCA	
		Pos.	Neg.
CTA	Pos.	True Pos. <b>107</b>	False Pos. <b>40</b>
	Neg.	False Neg. <b>22</b>	True Neg. <b>457</b>

n(Pat.)= 70  
 n(Seg.)= 626  
 n(Sten.)= 129

Sensitivity:	<b>0.83</b>
Specificity:	<b>0.92</b>
Pos. pred. Value:	<b>0.73</b>
Neg. pred. Value:	<b>0.95</b>

Fig. 29. Sensitivity, specificity, positive and negative predictive value for MDCT detection of coronary stenoses greater than 50% diameter of vessel lumen in all coronary segments.

		CCA	
		Pos.	Neg.
CTA	Pos.	True Pos. <b>107</b>	False Pos. <b>40</b>
	Neg.	False Neg. <b>39</b>	True Neg. <b>583</b>

n(Pat.)= 70  
 n(Seg.)= 769  
 n(Sten.)= 146

Sensitivity:	<b>0.73</b>
Specificity:	<b>0.94</b>
Pos. pred. Value:	<b>0.73</b>
Neg. pred. Value:	<b>0.94</b>

#### 4.6. Prospects of coronary CTA

This study demonstrates the high potential of CTA as a diagnostic tool for CAD. Yet, there are many obstacles that must be overcome if coronary CTA is to become a standard procedure. The major interfering factors in coronary CTA are cardiac motion and the small size of coronary vessels. A further increase of spatial and temporal resolution is necessary to overcome these obstacles and produce consistent results for proximal as well as for distal coronary segments. The development in MDCT technology has been very rapid in recent years, and newer scanner generations offer significantly higher temporal resolution achieved by faster gantry rotation time. The major limiting factors for further increasing gantry rotation times are the physical G-force at high rotation speed and the very fast data transfer rate necessary at shorter acquisition times (34). With the present technology an increase of spatial resolution may be achieved by thinner collimation, but this invariably causes an undesirable increase of radiation dose to the patient. A feasible approach to reduction of the patient dose is ECG-dependant tube modulation (ECG-pulsing). This method reduces the effective dose by varying the tube current according to the recorded ECG-trace of the patient. Full tube current is only needed during the diastole of the cardiac cycle since only data from this phase is used for image reconstruction. A significant reduction of patient dose is feasible with this method (34,35,38,45,54,99).

The apex of the rapid technical development seen in recent years has surely not yet been reached and further progress is to be expected. If the ongoing development in CT technology succeeds to diminish the challenges of coronary imaging, CTA has the potential of becoming a reliable non-invasive tool for the detection of CAD.

## 5. Summary

The objective of this study was to investigate the potential of high resolution four-row MDCT coronary angiography with retrospective ECG-gating for the detection of coronary artery stenoses. This was achieved by comparing the method to a gold standard set by conventional invasive coronary angiography.

A total of 70 patients scheduled for CCA were examined with CTA 1 – 2 days prior to conventional coronary angiography.

All patients were examined with a MDCT scanner capable of acquiring 4 slices per gantry rotation.

Initially a native MDCT scan was performed with a detector collimation of  $4 \times 2.5$  mm. These images were used to determine the scan volume and for quantification of coronary calcification.

After intravenous injection of non-ionic contrast media the entire heart volume could be scanned within a single breath hold with a slice with of 1.25mm (of  $4 \times 1$ mm collimation). All images were reconstructed from the MDCT data sets using retrospective ECG-synchronized gating. Each coronary segment was analyzed for the presence or absence of coronary stenoses and the location and extent of each lesion was recorded.

The results of CTA were compared with those of CCA in order to determine sensitivity, specificity, positive and negative predictive value for the detection of coronary stenoses with four-row MDCT angiography.

Further data analyses were performed to demonstrate the potentially interfering influence of variations in lesion size, heart rate, coronary calcification and lesion location within the coronary tree. Additionally, the influence of iodinated contrast media on mean patient heart rate was analyzed.

A total of 420 proximal coronary segments (segment 1, 2, 5, 6, 7 and 11) were evaluated with conventional coronary angiography. Of these segments 406 (96%) could be evaluated with MDCT angiography. The remaining 14 segments could not be adequately depicted due to image artifacts. 41% of the distal coronary segments could not be adequately depicted in CTA.

The statistical analysis to determine MDCT performance for the detection of coronary lesions greater 50% of vessel diameter in proximal coronary segments yielded high values for sensitivity (0.89) and specificity (0.90). Positive and negative values were 0.73 and 0.96, respectively.

The further evaluations accounting for lesion size, heart rate, coronary calcification and lesion location within the coronary tree all revealed variations of MDCT angiography performance. These factors possess the potential of influencing the results of MDCT coronary angiography in a negative manner.

In order to demonstrate how the intravenous application of non-ionic contrast media might influence patient heart rate, a comparative analysis of the mean heart rates of the 70 patients during the native and the contrast enhanced scan was performed. No significant difference of heart rate could be determined ( $p < 0.05$ ), suggesting that the applied quantity of iodinated contrast media does not cause significant variations in patient heart rate.

The results presented in this study indicate a high potential of MDCT angiography with retrospective ECG-gating for the detection of coronary stenoses. If a further reduction of image artifacts caused by cardiac motion can be achieved, coronary CTA may establish itself as a sensitive and readily available modality for the non-invasive detection of CAD.

# 6. Appendage

## 6.1. Raw Data

The following charts contain the original data collected during the study.

Fig. A1 lists the age, gender, number of stenosed vessels, mean heart rate during native and contrast enhanced scan, calcium score and the number of segments that could be evaluated in CCA and CTA respectively for each of the 70 patients.

Fig. A2.1 – A2.4 show the spreadsheet used for recording the stenosed coronary segments detected with CCA as well as CTA. Each coronary vessel is represented in a separate chart. The lesions are classified by the extent of lumen narrowing determined by each diagnostic modality with separate columns for each possible combination of variables. Proximal and distal lesions are recorded in separate columns (proximal lesions presented in black figures, distal lesions presented in gray figures).

This classification of the data facilitates the statistical analysis since each single combination of variables (lesion size and lesion location) is represented in a separate column.

It must be noted that the lesions listed in these charts do not all represent true positive findings although they were all diagnosed with CAA as well as with CTA. For example, if a lesion was classified as < 50% with CTA and 50-70% with CCA. This lesion counts as a false negative if the threshold of stenosis is defined to be all lesions > 50%. This example demonstrates the importance of the exact classification of each finding.

Fig. A3.1 - A3.4 presents the lesions seen in only one of the two imaging modalities. By definition these lesions are either false positive or false negative. The false negative findings are divided into two groups. The first group contains the coronary lesions that were missed with CTA although the coronary segment could be evaluated. The second group contains lesions that were missed with CTA because the coronary segment could not be depicted with this imaging modality.

Again, each lesion is categorized according to extent of stenosis diagnosed with each modality. Each lesion is consequently recorded in separate columns accounting for lesion size and lesion location.

Fig. A4.1 and A4.2 lists the heart rate of each patient measured at 1 sec. intervals after scan begin for a duration of 20 sec. Each row represents the calculated values for an individual patient. Blank cells occur when the heart rate is below 60 beats per minute so that some 1 sec. intervals do not contain a single heart beat.

Fig. A1

Pat. Number	Age	Gender	Number of Stenosed Vessels	Mean Heart Rate Nat. Scan	Mean Heart Rate CTA Scan	Ca.-Score (Agatston)	Segments seen in CCA	Segments seen in CTA
1	46	Male	1	58	57	0.3	10	9
2	55	Male	0	56	59	159.5	11	9
3	67	Male	1	63	67	678.5	10	7
4	61	Male	4	42	43	291.8	11	10
5	48	Male	1	69	68	22.7	10	8
6	62	Male	3	46	44	3138.1	11	11
7	68	Male	0	64	70	0	10	8
8	54	Male	0	59	58	500.8	10	9
9	70	Female	0	80	79	31.4	10	5
10	65	Male	1	81	75	1177.8	11	9
11	59	Male	1	90	91	328.5	11	10
12	60	Male	2	67	66	89.4	11	11
13	73	Female	1	107	68	3.7	10	7
14	61	Male	1	78	81	86.6	11	7
15	61	Male	1	53	48	52.5	11	7
16	44	Male	0	69	57	0	10	7
17	72	Male	2	58	56	120.2	12	12
18	62	Male	1	66	67	0	10	8
19	71	Male	1	63	68	64.3	10	6
20	61	Male	2	50	51	278.3	10	10
21	67	Male	2	60	61	443	13	13
22	61	Male	0	66	77	0	10	7
23	37	Male	0	77	65	1	10	9
24	67	Male	3	57	59	1524	16	15
25	41	Male	3	59	57	6.7	13	12
26	47	Female	1	58	68	0	10	10
27	66	Male	3	51	47	1912.2	14	12
28	50	Male	2	61	72	650	15	12
29	66	Male	0	62	66	433.1	10	7
30	61	Male	3	58	53	1183.4	11	9
31	69	Female	1	59	58	97.9	10	10
32	47	Male	1	64	59	540.6	12	12
33	50	Male	0	64	67	0	10	8
34	57	Male	1	51	48	687.2	12	10
35	73	Male	3	66	64	656.2	13	12
36	70	Male	3	46	46	298.9	13	11
37	56	Male	2	46	51	68.5	11	9
38	33	Male	0	53	60	0	10	7
39	66	Female	0	76	75	28.6	10	9
40	64	Female	1	61	62	4.7	10	9
41	47	Male	2	70	70	6.1	12	8
42	59	Male	1	66	74	53	10	9
43	73	Female	1	58	62	876.6	10	9
44	38	Male	1	73	74	0	11	8
45	66	Male	1	52	57	106.6	11	8
46	66	Male	2	64	59	2211.8	13	12
47	58	Male	2	51	52	3.6	10	8
48	50	Male	1	49	59	13.7	12	10
49	58	Female	1	74	85	30.7	11	6
50	56	Male	3	53	53	152.2	11	9
51	60	Male	1	67	78	253.3	10	4
52	71	Male	0	60	66	523.5	10	10
53	63	Male	0	65	67	220.3	10	10
54	74	Male	3	77	56	364.6	10	10
55	69	Male	0	69	67	0	10	4
56	58	Male	0	70	69	4	10	7
57	47	Male	3	70	65	169.4	12	9
58	51	Male	1	74	54	227.4	10	10
59	57	Male	1	54	51	132	11	11
60	44	Female	0	92	92	0	10	7
61	69	Female	1	56	55	124.8	12	9
62	65	Male	2	53	52	273.4	11	10
63	67	Male	3	69	68	154.2	14	11
64	59	Male	1	58	58	153.5	11	6
65	71	Male	1	51	53	130.1	12	11
66	48	Male	2	72	73	159.1	11	8
67	69	Male	1	55	54	1112.3	11	9
68	76	Female	0	69	68	73.9	10	7
69	60	Female	0	53	56	0	10	7
70	71	Female	0	61	62	2.2	10	6



Fig. A2.1

CCA	RCA																
	<50%	<50%	<50%	50-70%	50-70%	50-70%	>70%	>70%	>70%								
CTA	<50%	50-70%	>70%	<50%	50-70%	>70%	<50%	50-70%	>70%								
1	1																
2																	
3																	
4					1												
5	1								1								
6					1				1								
7																	
8	1																
9																	
10																	
11	1																
12									1								
13									2								
14																	
15																	
16																	
17		1															
18																	
19					1				1								
20								1									
21									2								
22																	
23					1												
24									2								
25	1				1				1								
26																	
27									2								
28									1								
29																	
30	1								1								
31																	
32	1	1						1									
33																	
34																	
35									2								
36								2									
37																	
38																	
39																	
40																	
41									1								
42	1				1				1								
43	1																
44																	
45																	
46	1				1		1										
47	1																
48		1															
49																	
50					1												
51	1																
52																	
53																	
54									1								
55																	
56																	
57									1								
58																	
59																	
60																	
61																	
62					1												
63																	
64									1								
65																	
66					1				1								
67						1											
68																	
69																	
70																	
<b>Sum</b>	<b>12</b>	<b>0</b>	<b>3</b>	<b>0</b>	<b>0</b>	<b>0</b>	<b>0</b>	<b>10</b>	<b>0</b>	<b>1</b>	<b>0</b>	<b>0</b>	<b>1</b>	<b>3</b>	<b>1</b>	<b>23</b>	<b>0</b>

Fig. A2.2

CCA	LAD																	
	<50%	<50%	<50%	50-70%	50-70%	50-70%	>70%	>70%	>70%									
CTA	<50%	50-70%	>70%	<50%	50-70%	>70%	<50%	50-70%	>70%									
1	1			1														
2	1	1																
3									1									
4					2					1								
5	1																	
6						1			1									
7																		
8																		
9			1															
10									1									
11					1		1											
12																		
13																		
14									1	1								
15									1	1								
16	1																	
17									1									
18					1													
19	1																	
20									1									
21									1									
22																		
23																		
24									2									
25		1																
26									1									
27									1	3								
28									2									
29		1																
30	1																	
31	1								1									
32			1	2														
33																		
34					1	1				1								
35										2								
36						1	1											
37										1								
38																		
39	1	1																
40	1									1								
41										1								
42																		
43	1																	
44																		
45	1					1												
46		1																
47	1				1													
48	1			1		1												
49							1		1									
50									1	1								
51										1								
52	1																	
53																		
54								1										
55																		
56																		
57						3												
58			1															
59										1								
60																		
61								1		1								
62										2								
63								1		1								
64																		
65	1									1								
66	2																	
67			1															
68	2																	
69																		
70																		
Sum	19	4	1	1	3	2	1	1	6	7	2	1	1	0	2	3	28	7

Fig. A2.3

CCA CTA	LCX																	
	<50%	<50%	<50%	50-70%	50-70%	50-70%	>70%	>70%	>70%									
	<50%	50-70%	>70%	<50%	50-70%	>70%	<50%	50-70%	>70%									
1																		
2																		
3																		
4									1									
5																		
6						1												
7	1																	
8	1																	
9																		
10																		
11	1																	
12									1									
13																		
14																		
15																		
16																		
17																		
18																		
19																		
20																		
21																		
22																		
23																		
24									1									
25							1											
26																		
27																		
28																		
29																		
30									1 1									
31																		
32																		
33																		
34			1															
35																		
36																		
37									1									
38																		
39																		
40																		
41																		
42																		
43					1													
44																		
45																		
46									1									
47					1													
48	1	1																
49																		
50									1									
51																		
52																		
53																		
54						1												
55																		
56																		
57					1													
58																		
59																		
60																		
61																		
62																		
63																		
64																		
65																		
66	1																	
67																		
68	1																	
69	1																	
70																		
Sum	7	0	1	0	1	0	0	0	3	0	2	0	1	0	0	0	6	2

Fig. A2.4

CCA	LM																			
	<50%	<50%	<50%	50-70%	50-70%	50-70%	>70%	>70%	>70%											
CTA	<50%	50-70%	>70%	<50%	50-70%	>70%	<50%	50-70%	>70%											
1	1																			
2																				
3	1																			
4																				
5																				
6																				
7																				
8																				
9																				
10																				
11																				
12																				
13																				
14																				
15																				
16																				
17																				
18																				
19																				
20																				
21																				
22																				
23																				
24																				
25																				
26																				
27																				
28																				
29																				
30																				
31																				
32																				
33																				
34																				
35																				
36	1																			
37																				
38																				
39																				
40																				
41																				
42																				
43																				
44																				
45																				
46																				
47																				
48																				
49																				
50																				
51																				
52																				
53																				
54																				
55																				
56																				
57																				
58																				
59																				
60																				
61																				
62																				
63																				
64									1											
65																				
66																				
67																				
68																				
69																				
70																				
Sum	3	0	0	0	0	0	0	0	0	0	0	0	0	0	0	0	0	0	1	0

Fig. A3.1

CCA	RCA																				
	False Neg. (seen)			False Neg. (not seen)			False Pos.														
	<50%	50-70%	>70%	<50%	50-70%	>70%	0	0	0												
CTA	0	0	0	Not seen	Not seen	Not seen	<50%	50-70%	>70%												
1																					
2						1															
3																					
4																					
5																					
6																					
7																					
8																					
9																					
10								1													
11																					
12																					
13																					
14																					
15																					
16																					
17																					
18																					
19																					
20	1	1		1																	
21																					
22																					
23																					
24																					
25																					
26							1	1													
27																					
28																					
29																					
30																					
31	1																				
32																					
33																					
34								1													
35																					
36																					
37																					
38							1														
39																					
40									1												
41				1																	
42																					
43																					
44																					
45																					
46																					
47																					
48																					
49																					
50				1																	
51																					
52									1												
53																					
54																					
55																					
56																					
57																					
58				1																	
59																					
60									1												
61																					
62																					
63		1							1												
64																					
65																					
66																					
67																					
68																					
69																					
70									1												
Sum	1	1	2	0	3	1	0	0	0	0	0	0	0	1	1	2	0	3	0	4	1

Fig. A3.2

CCA	LAD																			
	False Neg. (seen)			False Neg. (not seen)			False Pos.													
	<50%	50-70%	>70%	<50%	50-70%	>70%	0	0	0											
CTA	0	0	0	Not seen	Not seen	Not seen	<50%	50-70%	>70%											
1																				
2																				
3																				
4																				
5																				
6																				
7																				
8																				
9									1											
10									1											
11																				
12								1												
13																				
14																				
15																				
16																				
17																				
18							1													
19																				
20																				
21					1															
22									1											
23									1											
24																				
25			1	1																
26																				
27																				
28																				
29							1													
30																				
31																				
32							1													
33																				
34																				
35																				
36																				
37																				
38							1													
39																				
40																				
41																				
42									1											
43																				
44																				
45																				
46								1												
47																				
48																				
49																				
50																				
51																				
52								1												
53									1											
54				1																
55																				
56								1												
57																				
58																				
59									1											
60								1												
61								1												
62																				
63																				
64																				
65																				
66																				
67																				
68																				
69																				
70									1											
Sum	0	0	0	1	0	2	0	1	0	1	0	1	0	1	4	0	4	3	6	1

Fig. A3.3

CCA	LCX																	
	False Neg. (seen)			False Neg. (not seen)			False Pos.											
	<50%	50-70%	>70%	<50%	50-70%	>70%	0	0	0									
CTA	0	0	0	Not seen	Not seen	Not seen	<50%	50-70%	>70%									
1																		
2																		
3																		
4																		
5																		
6						1												
7																		
8																		
9								1										
10																		
11																		
12																		
13																		
14																		
15																		
16																		
17	1	2																
18																		
19																		
20																		
21						1												
22																		
23																		
24																		
25																		
26																		
27			1															
28					1													
29																		
30																		
31																		
32																		
33																		
34									1									
35				1														
36			1	1	1													
37																		
38								1										
39								1										
40																		
41						1												
42									1									
43																		
44			1						1									
45																		
46					1	1												
47																		
48																		
49								2										
50									1									
51																		
52																		
53																		
54																		
55																		
56																		
57																		
58																		
59																		
60																		
61									1									
62								1										
63									1									
64																		
65																		
66				1														
67						1		1										
68						1												
69																		
70																		
Sum	1	2	0	3	3	2	1	3	1	4	1	7	0	0	3	0	2	0

Fig. A3.4

	LM																		
	False Neg. (seen)			False Neg. (not seen)			False Pos.												
	<50%	50-70%	>70%	<50%	50-70%	>70%	0	0	0										
CCA	0	0	0	Not seen	Not seen	Not seen	<50%	50-70%	>70%										
CTA																			
1																			
2																			
3																			
4	1																		
5																			
6																			
7																			
8																			
9																			
10																			
11																			
12																			
13																			
14																			
15																			
16																			
17																			
18																			
19																			
20																			
21																			
22																			
23																			
24																			
25																			
26																			
27																			
28									1										
29																			
30																			
31																			
32																			
33																			
34																			
35																			
36																			
37																			
38																			
39																			
40																			
41																			
42																			
43																			
44																			
45																			
46																			
47																			
48																			
49																			
50																			
51																			
52																			
53																			
54																			
55																			
56																			
57																			
58																			
59																			
60																			
61																			
62																			
63																			
64																			
65																			
66																			
67																			
68																			
69																			
70																			
Sum	1	0	0	0	0	0	0	0	0	0	0	0	0	0	0	0	0	1	0



Fig. A4.1

Heart Rate During Native Scan																				
Sec.	1	2	3	4	5	6	7	8	9	10	11	12	13	14	15	16	17	18	19	20
1	70	61	58	57	57	58	58		58	58	58	55	56	55	56	58	58	59	59	58
2	56	59	58	55	56	54	53	54	56	56	57	58	57		57	56	54	54	56	53
3	66	63	61	54	58	60	61	63	65	62	65	65	65	65	65	66	65	68	64	67
4		46	44		43	42	41		41	41		41	42		41	41	41		42	42
5	71	71	70	69	69	68	68	69	69	69	68	68	68	67	67	68	68	68	69	70
6	45	39	61	51		47	49	47	46		45	44	44		43	42		42	42	42
7	54	61	62	61	62	62	62	63	63	65	65	65	65	65	65	65	65	66	68	68
8	65	59	57	57	57	57	58	58	59	59	61	59	60	60	59	60	59	59	58	58
9	77	73	73	76	78	80	82	83	86	84	84	83	81	82	78	80				
10	85	59	79	80	109	57	77	78	79	107	57	83	75	136	68	71	78	108	61	75
11	95	86	94	109	93	106	98	77	54	65	82	92	73	106	93	107	108			
12	67	66	65	65	65	65	67	67	67	68	68	68	68	69	68	67	68	67	67	67
13	77	73	65	96	63	129	101	135	132	89	161	130	106	106	89	117	79	94	131	161
14	86	78	74	76	78	78	77	76	77	79	76	78	77	78	79	79	80	79	82	
15	54	52	52	52	52		51	51	80		43	49	51	52	52		52	53	52	52
16	68	52	49	51	54	59	65	70	73	75	76	77	78	79	79	76	77	76	78	73
17	57	58	57	57	57	57	57	58	58	58	58	58	58	58	58	58	57	57	57	58
18	73	66	64	63	63	65	66	65	66	68	68	68	69	68	70	68	66	65	63	61
19	72	71	68	66	67	33	69	70	70		24			24	75	74	74	74	75	
20	54	53	52	49	49		49	48	49	49		48	48	48	49	50		51	52	52
21	57	57	57	58	58	57	58	58	59	61	61	61	61	61	62	61	61	63	62	61
22	69	68	67	66	65	65	65	65	65	65	65	65	65	65	66	66	66	65	65	63
23	67	68	70	71	72	73	73	75	78	78	81	84	81	80	79	79	78	82	82	83
24		58	49	43	59	50		61	59	63		51	47	63	43	57	50	63	55	95
25	54	55	57	58	58	60	60	61	61	61	61	61	62	61	59	59	59	59	60	59
26	66	62	59	55	57	59	57	58	58		50	57	52	54	57	58	61	59	59	59
27	53	51	50		50	49	49	49		49	49	51	51	51	51		51	51	52	52
28	65	62	61	61	61	61	61	61	63	64	62	62	61	59	61	61	60	61	61	61
29	103	104	59	58	57	58	57	57	57	57	57	58	58	57		57	56	56	60	54
30	56	56	57	57	57	57	58	59	59	60	60	61	59	59	58	59	57		57	57
31	60	59	59	58	60	60	59	58	60	59	59	58	59	59	59	59	58	57	58	58
32	59	60	61	63	62	63	65	67	68	65	65	65	66	65	65	65	65	64	67	66
33	61	61	61	61	62	62	63	64	64	63	63	63	62	65	64	66	66	66	68	71
34	49	49		50	50	51	51	51	51		50	51	52	51	52	51		52	51	52
35	64	65	65	65	65	66	65	65	65	65	64	64	64	65	65	64	65	107	51	64
36	49	42		43	44	44		45	46	46	46		47	48	48	49		48	49	
37		47	45	44		44	46	46		46	46	46		46	47	47	47		47	48
38	46		47	48	48	50	52		52	52	54	53	55	55	56	56	56	56	56	55
39		66	77	77	76	75	127	54	74	77	76	75	74	74	74	75	74	74		
40	55	55		57	57	58	59	60	61	63	64	65	64	64	64	63	63	63	63	64
41	63	62	63	65	67	69	70	71	73	73	73	71	71	72	72	73	75	76	74	76
42	72	72	69	68	66	66	66	65	67	65	67	65	65	65	67	65	65	65	64	63
43	60	57		57	56	57	59	59	60	61	59	59	60	58	58	56	57	57	56	57
44	87	77	72	69	72	73	75	73	71	73	67	72	69	70	69					
45		50	50	51	51	51	52	52		52	53	54	53	53	53	52		53	53	53
46	63	62	63	63	63	64	63	64	64	63	63	63	64	64	63	64	65	64	65	66
47	51		50	50	50	50	51		51	52	51	51	51	51		50	50	50	50	52
48	55	48	47	47		49	50	50	52	51	50		50	48	48	47	47	47	49	47
49	75	72	73	73	73	73	72	72	73	74	74	74	75	76	76	77	77	77		
50	57	45	49		51	57	59	58	47	50	50	57		51	53	54	55	54	54	55
51	70	71	68	68	65	65	65	65	66	65	67	68	65	68	68	67	68	66	67	65
52				12	59	62	60	60	61	61	62	63	63	64	64	65	65	65	65	64
53	67	63	61	62	62	62	62	63	64	65	66	67	68	68	69	68	67	67	67	68
54	65	52	54	159	58	58	61	52	66	53	73	66	55	173	90	66	70	63	69	145
55	72	70	70	69	68	69	68	69	68	68	69	70	70	69	70	69	69	69		
56	83	74	69	68	67	66	65	65	68	65	67	68	69	70	72	73	72	73	72	
57	73	71	69	70	71	71	71	70	70	70	69	70	68	68	68	68	68	69	69	67
58	53	52	51	52	53	48	56		51	49	156	57	49	53		60	181	52	133	124
59	55	56	56	55	54	53	53		53	53	53	52	52	53	53	54		53	52	53
60	98	90	91	95	94	93	92	92	91	89	91	89	89	90	89	92	92	94	99	97
61	49	56	57		56	57	57	57	56	57	57	57	56	57	58	57	57	57	57	57
62	54	52	52	51		53	52	52	53	53	54	54	53		53	53	53	53	54	55
63	70	69	69	91	54	63	65	67	68	99	55	66	68	68	68	69	68	68	68	68
64	57	56	55	55		57	55	56	57	57	58	59	58	62	59	58	58	59	65	63
65	54	54	54	53	45		47	48	49	50		50	56	56	54	52	47	49		50
66	76	78	75	73	73	71	71	70	70	71	70	70	70	68	69	70	71	72	72	70
67		53	54	54	55	54	54	55	55	55	56	55		56	55	56	55	57		
68	72	68	66	68	68	68	67	65	66	68	67	68	68	68	70	72	72	73	72	72
69	55	54	53	52	52	52	54	54		54	53	53	53	52	51	50		51	52	51
70	59	56	56	57	58	59	59	60	61	61	61	61	61	63	64	65	64	66	66	67

Fig. A4.2

Heart Rate During Contrast Enhanced Scan																				
Sec.	1	2	3	4	5	6	7	8	9	10	11	12	13	14	15	16	17	18	19	20
1	63	58	55	54	53	54	54	55	54		54	54	55	57	58	59	60	61	61	62
2	58	59	61		59	58	57	57	57	57	57	58	58	58	58	59	59	60	61	61
3	71	67	66	65	65	65	66	65	64	65	67	66	66.5	68	67	66	68	68	67	71
4		43	46	43		43	42	42		43	42		42	42	41		42	43		42
5	72	70	68	68	68	68	68	69	70	69	70	68	68	68	67	68	68	67	68	67
6	41	45	41	72	46		43	43		41	41		41	41	40		40	41		41
7	69	63	71	61	68	66	64	72	71	72	72	72	71	70	70	73	73	74	75	77
8	53	60	57	55	55	55	56	57	57	58	59	59	57	62	59	59	59	58	58	59
9	80	75	72	72	72	73	76	77	78	80	80	82	82	82	82	80	83	84	83	84
10	73	67	68	68	69	69	68	70	69	69	70	72	71	71	72	70	72	127	54	122
11	97	85	76	83	82	86	85	85	74	112	93	67	112	93	105	83	101	93	107	105
12	65	65	63	62	63	64	65	65	65	66	67	68	68	70	68	68	66	66	66	65
13	69	68	68	86		49	58	65	82	99	59	66	65	66	67	84		49	59	68
14	77	76	74	76	77	77	78	76	77	77	80	83	84	86	86	88	86	88	91	90
15	54	54	51	49	47		46	46	45		46	47	47	47		48	48	48	49	
16		53	48	47	49		50	50	53	55	57	58	62	61	60	62	69	70	63	61
17	59		55	54	54	54	54	55	55	55	56	55	56	55		56	57	57	57	57
18	73	80	74	68	63	61	62	62	62	63	65	66	69	68	67	68	67	66	66	66
19	73	72	69	33	66	64	65	65	66	67	69	69	71	72	73	73	73	73	75	74
20	53	51	50	52	52		50	49	48	50	51		52	53	53	52	51	51	52	52
21	61	59	58	59	58	58	59	59	59	60	61	63	62	62	65	64	65	65	65	65
22	72	85	64	72	73	73	74	74	72	74	74	75	77	78	79	80	82	84	86	85
23	72	73	73	70	66	64	61	61	60	60	57	55	59	61	65	66	66	67	68	66
24	78	72	72	66	65	61	49	41	54	49	63	75		43	56	47	54	60	54	68
25	51	51	54	55	58	59	59	60	61	61	62	61	60	60	58	56	55		55	56
26	71	69	68	67	64	63	65	66	67	66	67	67	68	68	69	72	70	71	71	72
27		29			26	51	50	50	50		51	51	50	50	50		50	50	50	50
28	77	69	68	67	67	68	67	68	69	71	70	71	71	72	73	74	75	77	77	79
29	57	56	57	55	57	112	76	58	58	59	59	59	106	80		58	56	56	57	81
30	55	53	53	53	53	53		52	53	53	52	52	52	51		51	51	53	53	55
31		58	57	55	56	57	57	57	58	58	58	59	59	58	59	60	59	61	61	61
32	54	53	53	54	56	57	57	58	58	61	61	61	61	62	64	65	63	63	63	63
33	67	68	68	67	68	67	65	65	63	63	63	64	67	68	68	68	68	68	68	68
34	51	47	47	47	47		47	47	47	47		48	48	47	49		49	49	49	50
35	64	64	63	63	62	63	63	64	64	64	65	64	65	64	64	65	65	65	65	65
36	45	45		44	39	46		47	51	43	45		45	45	44		47	48	50	49
37	86		35	49	49	95	34		49	49	49	48		46	46	44		44	45	45
38	62	68	63	55	52	53	54		51	52	54	57	61	62	61	61	63	63	66	73
39	69	68	68	68	69	69	69	72	72	72	74	73	73	74	75	133	64	80	79	79
40	68	58	56	54	54	55	58	60	61	61	63	62	63	63	64	65	65	66	68	68
41	73	66	65	65	65	65	67	66	68	71	72	72	72	72	73	72	71	72	72	73
42	73	72	72	70	70	68	69	70	71	72	73	74	75	77	79	78	78	79	80	80
43	65	63	62	61	63	63	65	63	65	65	66	65	65	65	67	73				13
44	86	76	72	72	73	75	72	77	72	72	72	71	74	73	72	73	72	73	73	73
45	53	56	56	56	56	57	56	56	58	62	59	58	58	57	58	57	57	58	58	59
46	61	61	60	59	59	59	58	57	57	58	58	59	58	58	59	59	59	60	61	60
47	53	52	53	51	51	51		51	51	52	52	52	52	53		53	53	54	53	54
48	54	52	52	53	54	56	57	58	58	57	59	59	61	60	61	63	65	65	69	72
49	79	80	81	80	83	83	85	87	101	81	83	101	79	84	85	88	85	84	85	85
50	57	58		53	52	54	53	53	53	53	53		52	52	52	53	52	49	52	
51	75	78	81	80	78	78	77	78	77	76	75	77	77	77	78	77	77	78	79	81
52	119	117			16	61	60	59	58	61	62	62	63	62	63	65	64	65	65	65
53	68	67	64	64	64	64	65	64	64	65	65	66	67	69	70	71	69	69	72	73
54	57	53		53	58	49	53	53	57	54	56	55	57	57		58	57	57	58	63
55	72	73	69	68	69	66	63	64	65	65	66	65	65	65	66	65	65	67	69	68
56	74	72	70	69	67	66	65	65	65	67	66	68	68	70	70	73	71	72	72	72
57	65	65	64	65	66	68	67	66	65	67	65	65	65	65	64	64	64	64	66	67
58	55	52	52	51		51	53	53	53	54	53	54	54	54		54	57	56	57	57
59	56	56	56	54	52	53	51	51		51	51	51	50	48		49	48	49	49	49
60	98	95	88	88	87	85	86	86	88	88	89	92	92	92	94	95	96	99	99	98
61	53		53	53	54	53	54	54	56	55	54	55		56	54	56	55	55	55	55
62	55	49		50	51	51	52	52	53	53		53	53	53	53	53	52	53	52	52
63	70	71	68	100	53	63	65	65	65	66	67	67	68	68	68	68	68	68	68	69
64	56	54	54	56	54	54		55	55	55	56	56	57	61	60	61	65	65	64	64
65	54	57	57		51	51	51	50	52	52		53	54	52	53	54	53	54	56	57
66	74	72	72	70	71	73	73	72	73	73	73	73	72	73	72	72	73	74	76	78
67	54	54	54	54		53	53	53	53	54	53	54	54	54		55	56	56	57	57
68	76	72	68	64	64	65	65	65	64	65	65	65	67	68	70	71	73	72	73	73
69	57	56	53	52		52	52	53	54	55	55	57	57	57	58	58	59	59	61	61
70	65	58	57	58	59	59	59		59	59	59	59	60	63	64	65	66	66	68	68

## 7. References

1. Achenbach S, Moshage W, Bachmann K. (1996)  
Coronary angiography by electron beam tomography.  
*Herz*, 21, 106-117.
2. Achenbach S, Moshage W, Ropers D, Bachmann K. (1998)  
Comparison of vessel diameters in electron beam tomography and quantitative coronary angiography.  
*Int J Card Imaging*, 14, 1-7; discussion 9.
3. Achenbach S, Moshage W, Ropers D, Nossen J, Daniel WG. (1998)  
Value of electron-beam computed tomography for the noninvasive detection of high-grade coronary-artery stenoses and occlusions.  
*N Engl J Med*, 339, 1964-1971.
4. Achenbach S, Ropers D, Holle J, Muschiol G, Daniel WG, Moshage W. (2000)  
In-plane coronary arterial motion velocity: measurement with electron-beam CT.  
*Radiology*, 216, 457-463.
5. Achenbach S, Ropers D, Mohlenkamp S, Schmermund A, Muschiol G, Groth J, Kusus M, Regenfus M, Daniel WG, Erbel R, Moshage W. (2001)  
Variability of repeated coronary artery calcium measurements by electron beam tomography.  
*Am J Cardiol*, 87, 210-213, A218.
6. Achenbach S, Giesler T, Ropers D, Ulzheimer S, Anders K, Wenkel E, Pohle K, Kachelriess M, Derlien H, Kalender WA, Daniel WG, Bautz W, Baum U. (2003)  
Comparison of image quality in contrast-enhanced coronary-artery visualization by electron beam tomography and retrospectively electrocardiogram-gated multislice spiral computed tomography.  
*Invest Radiol*, 38, 119-128.
7. Agatston AS, Janowitz WR, Hildner FJ, Zusmer NR, Viamonte M, Jr., Detrano R. (1990)  
Quantification of coronary artery calcium using ultrafast computed tomography.  
*J Am Coll Cardiol*, 15, 827-832.
8. AHA. (1999)  
American Heart Association Committee Report. A reporting system on patients evaluated for coronary artery disease.  
*Circulation*, 51, 7-34.

9. Altman DG, Gardner MJ. (1988)  
Calculating confidence intervals for regression and correlation.  
*Br Med J (Clin Res Ed)*, 296, 1238-1242.
10. Assmann G. (1988)  
European Consensus on Primary Prevention of Coronary Heart Disease.  
*Can J Cardiol*, 4 Suppl A, 21A-23A.
11. Assmann G, Carmena R, Cullen P, Fruchart JC, Jossa F, Lewis B, Mancini M, Paoletti R. (1999)  
Coronary heart disease: reducing the risk: a worldwide view.  
International Task Force for the Prevention of Coronary Heart Disease.  
*Circulation*, 100, 1930-1938.
12. Becker C, Schatzl M, Feist H, Bauml A, Schopf UJ, Michalski G, Lechel U, Hengge M, Bruning R, Reiser M. (1999)  
[Assessment of the effective dose for routine protocols in conventional CT, electron beam CT and coronary angiography].  
*Röfo Fortschr Geb Rontgenstr Neuen Bildgeb Verfahr*, 170, 99-104.
13. Becker CR, Jakobs T, Knez A, Becker A, Haberl R, Bruning R, Schoepf UJ, Reiser MF. (1998)  
[Methods of quantification of coronary artery calcifications with electron-beam and conventional computed tomography].  
*Radiologe*, 38, 1006-1011.
14. Becker CR, Knez A, Jakobs TF, Aydemir S, Becker A, Schoepf UJ, Bruening R, Haberl R, Reiser MF. (1999)  
Detection and quantification of coronary artery calcification with electron-beam and conventional CT.  
*Eur Radiol*, 9, 620-624.
15. Becker CR, Knez A, Ohnesorge B, Schoepf UJ, Flohr T, Bruening R, Haberl R, Reiser MF. (2000)  
Visualization and quantification of coronary calcifications with electron beam and spiral computed tomography.  
*Eur Radiol*, 10, 629-635.
16. Bostrom K. (2001)  
Insights into the mechanism of vascular calcification.  
*Am J Cardiol*, 88, 20E-22E.
17. Budoff MJ, Georgiou D, Brody A, Agatston AS, Kennedy J, Wolfkiel C, Stanford W, Shields P, Lewis RJ, Janowitz WR, Rich S, Brundage BH. (1996)  
Ultrafast computed tomography as a diagnostic modality in the detection of coronary artery disease: a multicenter study.  
*Circulation*, 93, 898-904.

18. Burke AP, Farb A, Malcom GT, Liang Y, Smialek J, Virmani R. (1998)  
Effect of risk factors on the mechanism of acute thrombosis and sudden coronary death in women.  
*Circulation*, 97, 2110-2116.
19. Burke AP, Weber DK, Kolodgie FD, Farb A, Taylor AJ, Virmani R. (2001)  
Pathophysiology of calcium deposition in coronary arteries.  
*Herz*, 26, 239-244.
20. Burke AP, Kolodgie FD, Farb A, Weber D, Virmani R. (2002)  
Morphological predictors of arterial remodeling in coronary atherosclerosis.  
*Circulation*, 105, 297-303.
21. Callister TQ, Cooil B, Raya SP, Lippolis NJ, Russo DJ, Raggi P. (1998)  
Coronary artery disease: improved reproducibility of calcium scoring with an electron-beam CT volumetric method.  
*Radiology*, 208, 807-814.
22. Challande P, Plainfosse MC. (1994)  
Reliability of coronary calcium quantification with electron beam CT.  
*Radiology*, 193, 282-283.
23. Chernoff DM, Ritchie CJ, Higgins CB. (1997)  
Evaluation of electron beam CT coronary angiography in healthy subjects.  
*AJR Am J Roentgenol*, 169, 93-99.
24. Choi HS, Choi BW, Choe KO, Choi D, Yoo KJ, Kim MI, Kim J. (2004)  
Pitfalls, artifacts, and remedies in multi-detector row CT coronary angiography.  
*Radiographics*, 24, 787-800.
25. Chung CS, Karamanoglu M, Kovacs SJ. (2004)  
Duration of diastole and its phases as a function of heart rate during supine bicycle exercise.  
*Am J Physiol Heart Circ Physiol*, 287, H2003-2008.
26. Cleland JG, Swedberg K, Cohen-Solal A, Cosin-Aguilar J, Dietz R, Follath F, Gavazzi A, Hobbs R, Korewicki J, Madeira HC, Preda I, van Gilst WH, Widimsky J, Mareev V, Mason J, Freemantle N, Eastaugh J. (2000)  
The Euro Heart Failure Survey of the EUROHEART survey programme. A survey on the quality of care among patients with heart failure in Europe.  
*Eur J Heart Fail*, 2, 123-132.

27. Cullen P, Schulte H, Assmann G. (1998)  
Smoking, lipoproteins and coronary heart disease risk. Data from the Munster Heart Study (PROCAM).  
*Eur Heart J*, 19, 1632-1641.
28. Farb A, Tang AL, Burke AP, Sessums L, Liang Y, Virmani R. (1995)  
Sudden coronary death. Frequency of active coronary lesions, inactive coronary lesions, and myocardial infarction.  
*Circulation*, 92, 1701-1709.
29. Farb A, Burke AP, Tang AL, Liang TY, Mannan P, Smialek J, Virmani R. (1996)  
Coronary plaque erosion without rupture into a lipid core. A frequent cause of coronary thrombosis in sudden coronary death.  
*Circulation*, 93, 1354-1363.
30. Feltrin GP, Zandona M, Borile V, Rettore C, Miotto D. (2004)  
[Fundamentals on iodinated contrast media and adverse reactions].  
*Radiol Med (Torino)*, 107, 8-31.
31. Ferencik M, Moselewski F, Ropers D, Hoffmann U, Baum U, Anders K, Pomerantsev EV, Abbara S, Brady TJ, Achenbach S. (2003)  
Quantitative parameters of image quality in multidetector spiral computed tomographic coronary imaging with submillimeter collimation.  
*Am J Cardiol*, 92, 1257-1262.
32. Fleischmann D, Rubin GD, Paik DS, Yen SY, Hilfiker PR, Beaulieu CF, Napel S. (2000)  
Stair-step artifacts with single versus multiple detector-row helical CT.  
*Radiology*, 216, 185-196.
33. Flohr T, Ohnesorge B. (2001)  
Heart rate adaptive optimization of spatial and temporal resolution for electrocardiogram-gated multislice spiral CT of the heart.  
*J Comput Assist Tomogr*, 25, 907-923.
34. Flohr T, Küttner A, Bruder H, Stierstorfer K, Halliburton SS, Schaller S, Ohnesorge BM. (2003)  
Performance evaluation of a multi-slice CT system with 16-slice detector and increased gantry rotation speed for isotropic submillimeter imaging of the heart.  
*Herz*, 28, 7-19.
35. Flohr TG, Schoepf UJ, Küttner A, Halliburton S, Bruder H, Suess C, Schmidt B, Hofmann L, Yucel EK, Schaller S, Ohnesorge BM. (2003)  
Advances in cardiac imaging with 16-section CT systems.  
*Acad Radiol*, 10, 386-401.

36. Gardner MJ, Altman DG. (1986)  
Confidence intervals rather than P values: estimation rather than hypothesis testing.  
*Br Med J (Clin Res Ed)*, 292, 746-750.
37. Georg C, Kopp A, Schroder S, Küttner A, Ohnesorge B, Martensen J, Clausen CD. (2001)  
[Optimizing image reconstruction timing for the RR interval in imaging coronary arteries with multi-slice computerized tomography].  
*Röfo Fortschr Geb Rontgenstr Neuen Bildgeb Verfahr*, 173, 536-541.
38. Gies M, Kalender WA, Wolf H, Suess C. (1999)  
Dose reduction in CT by anatomically adapted tube current modulation. I. Simulation studies.  
*Med Phys*, 26, 2235-2247.
39. Giesler T, Baum U, Ropers D, Ulzheimer S, Wenkel E, Mennicke M, Bautz W, Kalender WA, Daniel WG, Achenbach S. (2002)  
Noninvasive visualization of coronary arteries using contrast-enhanced multidetector CT: influence of heart rate on image quality and stenosis detection.  
*AJR Am J Roentgenol*, 179, 911-916.
40. Graf H, Heuschmid M, Küttner A, Kopp AF, Claussen CD, Schick F. (2002)  
[Characterization of motion artifacts in multi-slice spiral CT].  
*Röfo Fortschr Geb Rontgenstr Neuen Bildgeb Verfahr*, 174, 1301-1308.
41. Greenland P, Abrams J, Aurigemma GP, Bond MG, Clark LT, Criqui MH, Crouse JR, 3rd, Friedman L, Fuster V, Herrington DM, Kuller LH, Ridker PM, Roberts WC, Stanford W, Stone N, Swan HJ, Taubert KA, Wexler L. (2000)  
Prevention Conference V: Beyond secondary prevention: identifying the high-risk patient for primary prevention: noninvasive tests of atherosclerotic burden: Writing Group III.  
*Circulation*, 101, E16-22.
42. Guyatt G, Jaeschke R, Heddle N, Cook D, Shannon H, Walter S. (1995)  
Basic statistics for clinicians: 2. Interpreting study results: confidence intervals.  
*Cmaj*, 152, 169-173.
43. Haberl R, Knez A, Becker A, Becker C, Maass A, Bruning R, Reiser M, Steinbeck G. (1998)  
[Significance of calcium detection with electron-beam tomography in coronary disease].  
*Radiologe*, 38, 999-1005.

44. Harris EK. (1993)  
On P values and confidence intervals (why can't we P with more confidence?).  
*Clin Chem*, 39, 927-928.
45. Herzog P, Jakobs TF, Wintersperger BJ, Nikolaou K, Becker CR, Reiser MF. (2002)  
[Radiation dose and dose reduction in multidetector row CT (MDCT)].  
*Radiologe*, 42, 691-696.
46. Hong C, Becker CR, Huber A, Schoepf UJ, Ohnesorge B, Knez A, Bruning R, Reiser MF. (2001)  
ECG-gated reconstructed multi-detector row CT coronary angiography: effect of varying trigger delay on image quality.  
*Radiology*, 220, 712-717.
47. Hong C, Bae KT, Pilgram TK, Zhu F. (2003)  
Coronary artery calcium quantification at multi-detector row CT: influence of heart rate and measurement methods on interacquisition variability initial experience.  
*Radiology*, 228, 95-100.
48. Huang H, Virmani R, Younis H, Burke AP, Kamm RD, Lee RT. (2001)  
The impact of calcification on the biomechanical stability of atherosclerotic plaques.  
*Circulation*, 103, 1051-1056.
49. Janowitz WR. (2000)  
Coronary calcium does not accurately predict near-term future coronary events in high-risk adults.  
*Circulation*, 102, E20-21.
50. Janowitz WR. (2001)  
Current status of mechanical computed tomography in cardiac imaging.  
*Am J Cardiol*, 88, 35E-38E.
51. Kalender W. (2000)  
Computer-tomographie.  
*Publics MCD Verlag*, 1. Edition.
52. Kalender WA. (1994)  
Technical foundations of spiral CT.  
*Semin Ultrasound CT MR*, 15, 81-89.
53. Kalender WA. (1994)  
Principles and applications of spiral CT.  
*Nucl Med Biol*, 21, 693-699.



54. Kalender WA, Wolf H, Suess C. (1999)  
Dose reduction in CT by anatomically adapted tube current modulation. II. Phantom measurements.  
*Med Phys*, 26, 2248-2253.
55. Keelan PC, Bielak LF, Ashai K, Jamjoum LS, Denktas AE, Rumberger JA, Sheedy IP, Peyser PA, Schwartz RS. (2001)  
Long-term prognostic value of coronary calcification detected by electron-beam computed tomography in patients undergoing coronary angiography.  
*Circulation*, 104, 412-417.
56. Kennedy JW. (1982)  
Complications associated with cardiac catheterization and angiography.  
*Cathet Cardiovasc Diagn*, 8, 5-11.
57. Kondos GT, Hoff JA, Sevrakov A, Daviglius ML, Garside DB, Devries SS, Chomka EV, Liu K. (2003)  
Electron-beam tomography coronary artery calcium and cardiac events: a 37-month follow-up of 5635 initially asymptomatic low- to intermediate-risk adults.  
*Circulation*, 107, 2571-2576.
58. Kopp AF, Schroeder S, Baumbach A, Küttner A, Georg C, Ohnesorge B, Heuschmid M, Kuzo R, Claussen CD. (2001)  
Non-invasive characterisation of coronary lesion morphology and composition by multislice CT: first results in comparison with intracoronary ultrasound.  
*Eur Radiol*, 11, 1607-1611.
59. Kopp AF, Schroeder S, Küttner A, Heuschmid M, Georg C, Ohnesorge B, Kuzo R, Claussen CD. (2001)  
Coronary arteries: retrospectively ECG-gated multi-detector row CT angiography with selective optimization of the image reconstruction window.  
*Radiology*, 221, 683-688.
60. Kopp AF, Ohnesorge B, Becker C, Schroder S, Heuschmid M, Küttner A, Kuzo R, Claussen CD. (2002)  
Reproducibility and accuracy of coronary calcium measurements with multi-detector row versus electron-beam CT.  
*Radiology*, 225, 113-119.
61. Kracoff OH, Adelman AG. (1988)  
Heart rate response to intracoronary contrast media injection before and after percutaneous transluminal coronary angioplasty.  
*Am J Cardiol*, 61, 1117-1118.

62. Laroche D, Vergnaud MC, Lefrancois C, Hue S, Bricard H. (2002)  
Anaphylactoid reactions to iodinated contrast media.  
*Acad Radiol*, 9 Suppl 2, S431-432.
63. Lin YC, Shida KK, Hong SK. (1983)  
Effects of hypercapnia, hypoxia, and rebreathing on heart rate response during apnea.  
*J Appl Physiol*, 54, 166-171.
64. Martinelli G, Petrini F, Gamberini E. (2004)  
[Adverse reactions to contrast media: treatment].  
*Radiol Med (Torino)*, 107, 42-52.
65. Mautner SL, Mautner GC, Froehlich J, Feuerstein IM, Proschan MA, Roberts WC, Doppman JL. (1994)  
Coronary artery disease: prediction with in vitro electron beam CT.  
*Radiology*, 192, 625-630.
66. Medina LS, Zurakowski D. (2003)  
Measurement variability and confidence intervals in medicine: why should radiologists care?  
*Radiology*, 226, 297-301.
67. Mennicke M, Giesler T, Ropers D, Baum U, Ulzheimer S, Wenkel E, Pohle K, Daniel WG, Achenbach S. (2002)  
[Influence of heart rate on image quality and detection of coronary stenoses with multislice spiral CT].  
*Biomed Tech (Berl)*, 47 Suppl 1 Pt 2, 782-785.
68. Moshage WE, Achenbach S, Seese B, Bachmann K, Kirchgeorg M. (1995)  
Coronary artery stenoses: three-dimensional imaging with electrocardiographically triggered, contrast agent-enhanced, electron-beam CT.  
*Radiology*, 196, 707-714.
69. Naghavi M, Libby P, Falk E, Casscells SW, Litovsky S, Rumberger J, Badimon JJ, Stefanadis C, Moreno P, Pasterkamp G, Fayad Z, Stone PH, Waxman S, Raggi P, Madjid M, Zarrabi A, Burke A, Yuan C, Fitzgerald PJ, Siscovick DS, de Korte CL, Aikawa M, Airaksinen KE, Assmann G, Becker CR, Chesebro JH, Farb A, Galis ZS, Jackson C, Jang IK, Koenig W, Lodder RA, March K, Demirovic J, Navab M, Priori SG, Rehkter MD, Bahr R, Grundy SM, Mehran R, Colombo A, Boerwinkle E, Ballantyne C, Insull W, Jr., Schwartz RS, Vogel R, Serruys PW, Hansson GK, Faxon DP, Kaul S, Drexler H, Greenland P, Muller JE, Virmani R, Ridker PM, Zipes DP, Shah PK, Willerson JT. (2003)  
From vulnerable plaque to vulnerable patient: a call for new definitions and risk assessment strategies: Part II.  
*Circulation*, 108, 1772-1778.

70. Newman AB, Naydeck BL, Sutton-Tyrrell K, Feldman A, Edmundowicz D, Kuller LH. (2001)  
Coronary artery calcification in older adults to age 99: prevalence and risk factors.  
*Circulation*, 104, 2679-2684.
71. Nieman K, Cademartiri F, Lemos PA, Raaijmakers R, Pattynama PM, de Feyter PJ. (2002)  
Reliable noninvasive coronary angiography with fast submillimeter multislice spiral computed tomography.  
*Circulation*, 106, 2051-2054.
72. Nieman K, Rensing BJ, van Geuns RJ, Vos J, Pattynama PM, Krestin GP, Serruys PW, de Feyter PJ. (2002)  
Non-invasive coronary angiography with multislice spiral computed tomography: impact of heart rate.  
*Heart*, 88, 470-474.
73. Nossen J, Achenbach S, Moshage W, Ropers D, Daniel WG. (1998)  
[Evaluating trigger timing in detection and quantification of coronary artery calcinosis with electron beam tomography].  
*Biomed Tech (Berl)*, 43 Suppl, 50-51.
74. Ohnesorge B, Flohr T, Schaller S, Klingenbeck-Regn K, Becker C, Schopf UJ, Bruning R, Reiser MF. (1999)  
[The technical bases and uses of multi-slice CT].  
*Radiologe*, 39, 923-931.
75. Ohnesorge B, Flohr T, Becker C, Knez A, Kopp AF, Fukuda K, Reiser MF. (2000)  
[Cardiac imaging with rapid, retrospective ECG synchronized multilevel spiral CT].  
*Radiologe*, 40, 111-117.
76. Ohnesorge B, Flohr T, Becker C, Kopp AF, Schoepf UJ, Baum U, Knez A, Klingenbeck-Regn K, Reiser MF. (2000)  
Cardiac imaging by means of electrocardiographically gated multisection spiral CT: initial experience.  
*Radiology*, 217, 564-571.
77. Ohnesorge B, Becker CR, Flohr T, Reiser M. (2002)  
Multi-slice CT in Cardiac Imaging.  
*Springer-Verlag, Berlin, Heidelberg, New York*, 1. Edition.

78. Pasterkamp G, Schoneveld AH, van der Wal AC, Hijnen DJ, van Wolveren WJ, Plomp S, Teepen HL, Borst C. (1999)  
Inflammation of the atherosclerotic cap and shoulder of the plaque is a common and locally observed feature in unruptured plaques of femoral and coronary arteries.  
*Arterioscler Thromb Vasc Biol*, 19, 54-58.
79. Pasterkamp G, Schoneveld AH, Hijnen DJ, de Kleijn DP, Teepen H, van der Wal AC, Borst C. (2000)  
Atherosclerotic arterial remodeling and the localization of macrophages and matrix metalloproteases 1, 2 and 9 in the human coronary artery.  
*Atherosclerosis*, 150, 245-253.
80. Prokop M, Schaefer C, Kalender WA, Polacin A, Galanski M. (1993)  
[Vascular imaging with spiral-CT. The path to CT-angiography].  
*Radiologe*, 33, 694-704.
81. Rankin SC. (1998)  
Spiral CT: vascular applications.  
*Eur J Radiol*, 28, 18-29.
82. Rayner M, Peterson S. (2000)  
European Cardiovascular Disease Statistics.  
*British Heart Foundation Health Promotion Research Group, University of Oxford, Institute of Health Sciences*, 1, 2-15.
83. Rensing BJ, Bongaerts A, van Geuns RJ, van Ooijen P, Oudkerk M, de Feyter PJ. (1998)  
Intravenous coronary angiography by electron beam computed tomography: a clinical evaluation.  
*Circulation*, 98, 2509-2512.
84. Rubin GD, Shiau MC, Schmidt AJ, Fleischmann D, Logan L, Leung AN, Jeffrey RB, Napel S. (1999)  
Computed tomographic angiography: historical perspective and new state-of-the-art using multi detector-row helical computed tomography.  
*J Comput Assist Tomogr*, 23 Suppl 1, S83-90.
85. Scanlon PJ, Faxon DP, Audet AM, Carabello B, Dehmer GJ, Eagle KA, Legako RD, Leon DF, Murray JA, Nissen SE, Pepine CJ, Watson RM, Ritchie JL, Gibbons RJ, Chaitlin MD, Gardner TJ, Garson A, Jr., Russell RO, Jr., Ryan TJ, Smith SC, Jr. (1999)  
ACC/AHA guidelines for coronary angiography. A report of the American College of Cardiology/American Heart Association Task Force on practice guidelines (Committee on Coronary Angiography). Developed in collaboration with the Society for Cardiac Angiography and Interventions.  
*J Am Coll Cardiol*, 33, 1756-1824.

86. Schmermund A, Rensing BJ, Sheedy PF, Bell MR, Rumberger JA. (1998)  
Intravenous electron-beam computed tomographic coronary angiography for segmental analysis of coronary artery stenoses.  
*J Am Coll Cardiol*, 31, 1547-1554.
87. Schmermund A, Schwartz RS, Adamzik M, Sangiorgi G, Pfeifer EA, Rumberger JA, Burke AP, Farb A, Virmani R. (2001)  
Coronary atherosclerosis in unheralded sudden coronary death under age 50: histo-pathologic comparison with 'healthy' subjects dying out of hospital.  
*Atherosclerosis*, 155, 499-508.
88. Schoenhagen P, White RD, Nissen SE, Tuzcu EM. (2003)  
Coronary imaging: angiography shows the stenosis, but IVUS, CT, and MRI show the plaque.  
*Cleve Clin J Med*, 70, 713-719.
89. Schroeder S, Kopp AF, Baumbach A, Küttner A, Georg C, Ohnesorge B, Herdeg C, Claussen CD, Karsch KR. (2001)  
Non-invasive characterisation of coronary lesion morphology by multi-slice computed tomography: a promising new technology for risk stratification of patients with coronary artery disease.  
*Heart*, 85, 576-578.
90. Schroeder S, Kopp AF, Küttner A, Burgstahler C, Herdeg C, Heuschmid M, Baumbach A, Claussen CD, Karsch KR, Seipel L. (2002)  
Influence of heart rate on vessel visibility in noninvasive coronary angiography using new multislice computed tomography: experience in 94 patients.  
*Clin Imaging*, 26, 106-111.
91. Shaw LJ, Raggi P, Schisterman E, Berman DS, Callister TQ. (2003)  
Prognostic value of cardiac risk factors and coronary artery calcium screening for all-cause mortality.  
*Radiology*, 228, 826-833.
92. Shemesh J, Tenenbaum A, Fisman EZ, Apter S, Rath S, Rozenman J, Itzchak Y, Motro M. (1996)  
Absence of coronary calcification on double-helical CT scans: predictor of angiographically normal coronary arteries in elderly women?  
*Radiology*, 199, 665-668.
93. Silber S. (2003)  
[Early detection of myocardial infarct risk with cardio-CT. Can coronary calcium calculation prevention sudden cardiac death?].  
*MMW Fortschr Med*, 145, 37-40.

94. Stanford W, Burns TL, Thompson BH, Witt JD, Lauer RM, Mahoney LT. (2004)  
Influence of body size and section level on calcium phantom measurements at coronary artery calcium CT scanning.  
*Radiology*, 230, 198-205.
95. Sary HC. (2000)  
Natural history of calcium deposits in atherosclerosis progression and regression.  
*Z Kardiol*, 89 Suppl 2, 28-35.
96. Sary HC. (2000)  
Natural history and histological classification of atherosclerotic lesions: an update.  
*Arterioscler Thromb Vasc Biol*, 20, 1177-1178.
97. Sary HC. (2001)  
The development of calcium deposits in atherosclerotic lesions and their persistence after lipid regression.  
*Am J Cardiol*, 88, 16E-19E.
98. Taylor AJ, Burke AP, O'Malley PG, Farb A, Malcom GT, Smialek J, Virmani R. (2000)  
A comparison of the Framingham risk index, coronary artery calcification, and culprit plaque morphology in sudden cardiac death.  
*Circulation*, 101, 1243-1248.
99. Trabold T, Buchgeister M, Küttner A, Heuschmid M, Kopp AF, Schroder S, Claussen CD. (2003)  
Estimation of radiation exposure in 16-detector row computed tomography of the heart with retrospective ECG-gating.  
*Röfo Fortschr Geb Rontgenstr Neuen Bildgeb Verfahr*, 175, 1051-1055.
100. Vink A, Pasterkamp G. (2002)  
Atherosclerotic plaque burden, plaque vulnerability and arterial remodeling: the role of inflammation.  
*Minerva Cardioangiol*, 50, 75-83.
101. Vogl TJ, Abolmaali ND, Diebold T, Engelmann K, Ay M, Dogan S, Wimmer-Greinecker G, Moritz A, Herzog C. (2002)  
Techniques for the detection of coronary atherosclerosis: multi-detector row CT coronary angiography.  
*Radiology*, 223, 212-220.
102. Yoon HC, Goldin JG, Greaser LE, 3rd, Sayre J, Fonarow GC. (2000)  
Interscan variation in coronary artery calcium quantification in a large asymptomatic patient population.  
*AJR Am J Roentgenol*, 174, 803-809.

103. Yoshikawa H. (1992)  
Late adverse reactions to nonionic contrast media.  
*Radiology*, 183, 737-740.

# Acknowledgements

I would like to extend my gratitude to Professor C. D. Claussen, Department of Diagnostic Radiology, Eberhard-Karls-University Tübingen, who has promoted my work and placed his confidence in my ability.

PD Dr. Andreas Kopp has been a valuable advisor and mentor to me. His work has been a constant source of inspiration and his advice has eased the labor involved with the planning and execution of this thesis.

My work with Dr. Axel Küttner has been enjoyable and gratifying. He has always had an open ear for all problems and challenges and his advice has eased my labor considerably. Our work together has been rewarded with a personal friendship, for which I am grateful.

Mr. Meisner from the Institut of Medical Biometry, Eberhard-Karls-University Tübingen, has guided me through the challenges of statistical data analysis, which I could never have mastered without his help.

My warmest gratitude goes to my family and relatives who have supported me in every way possible. A special thanks goes to my father in law, Dr. Roman Weiske, who has been an invaluable source of support and inspiration to me.

Above all I thank my wife Romana for her unwavering support without which the completion of this thesis would not have been possible.



# Curriculum vitae

Name: Jens Martensen  
Born: 23. December 1975 in Hørsholm, Denmark.  
Marital status: Married to Romana Martensen-Weiske  
Citizenship: Danish

## School

1982 – 1991 Primary school („Folkeskole“) in Denmark  
1992 – 1994 John F. Kennedy High school, Sacramento  
1994 – 1996 Karlsgymnasium Stuttgart

## University

1996 Admission to Medical School, Eberhard-Karls-Universität  
Tübingen  
1997 „Physikum“  
1998 First Medical Exam in Tübingen  
2002 Second Medical Exam in Tübingen  
2003 Final Medical Exam in Tübingen, November 23, 2003

## Practical Training

1999 1. Clerkship, Kreiskrankenhaus Leonberg, surgical section  
1999 2. Clerkship, Universitätsklinik Tübingen, cardiological section  
2000 3. Clerkship, Radiological Associates of Sacramento  
2001 4. Clerkship, Stanford Medical School, department of radiology,  
cardiovascular section  
  
2002 1. Internship, Krankenhaus Bad Cannstatt Klinikum Stuttgart,  
surgical section  
2003 2. Internship, Brigham and Women’s Hospital, Harvard Medical  
School, department of radiology, thorasic imaging section  
2003 3. Internship, Krankenhaus Bad Cannstatt Klinikum Stuttgart,  
gastroenterological section

## Professional Training

Jan. 2004 Arzt in Praktikum, Kreiskrankenhaus Leonberg, department of  
internal medicine  
Okt. 2004 Assistenzarzt, Kreiskrankenhaus Leonberg, department of internal  
medicine